Structural Engineering Report No. 88

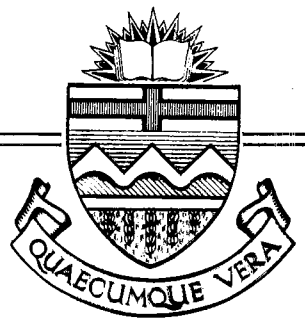

BEHAVIOR OF PRESTRESSED CONCRETE CONTAINMENT STRUCTURES A SUMMARY OF FINDINGS

by
J. G. MacGREGOR
D. W. MURRAY
and
S. H. SIMMONDS

May 1980

The University of Alberta

Department of Civil Engineering

Behavior of Prestressed Concrete Containment Structures

A Summary of Findings

by

J.G. MacGregor
D.W. Murray
S.H. Simmonds

A Technical Report to the
Atomic Energy Control Board
Nuclear Plant Licensing Directorate
P.O. Box 1046
Ottawa, Canada, K1P 5S9

May, 1980

ACKNOWLEDGEMENTS

The authors wish to acknowledge the cooperation of the following agencies which provided technical information and/or financial support for the overall study.

The Atomic Energy Control Board

Atomic Energy of Canada, Limited

Hydro-Quebec

Canatom Limited

Ontario-Hydro

DISCLAIMER

The interpretation of the technical data and any opinions or conclusions arising in this report are those of the authors only and do not necessarily reflect those of the co-operating agencies.

TABLE OF CONTENTS

LIST OF TABLES

LIST OF FIGURES

I. INTRODUCTION

1.1 Purpose and Results of the Study

The reactors in a Canadian nuclear power plant of the Gentilly-2 type are enclosed in a circular prestressed concrete structure. In the event of certain malfunctions in which pressurized gases or steam are discharged, this concrete enclosure acts as a containment structure to prevent these products from escaping into the atmosphere.

The largest internal pressures considered in design result from a complete rupture of a secondary steam line.The Gentilly-2 plant is designed so that the increased pressure due to this release of steam would activate a water dousing system which would cool and condense the steam, limiting the maximum internal pressure to 18.5 psi. This is referred to as the design basis accident. One of the design criteria for the containment is that there be no tensile stresses in the inner surfaces of the concrete under a pressure of 1.15 times this amount.

In the extremely unlikely event that a secondary steam line ruptures completely and simultaneously the dousing system fails to act, the internal pressure may reach several times the design pressure. The Atomic Energy Control Board of Canada sponsored a comprehensive study at the University of Alberta to determine the response of a containment structure to such overpressures.

As the internal pressure in a prestressed concrete containment structure increases, it is possible to postulate a series of stages of increasing damage to the structure which limit its usefulness. These conditions are referred to as "Limit

States" and include such states as first surface cracking, first through-the-wall cracking, initial yielding of reinforcement, first yielding of prestressing tendons, and fracture of reinforcement and/or tendons. The objectives of the study were to develop a methodology that would permit the prediction of both the internal pressure and locations in the containment where these limit states occur and the estimation of the rate of leakage through the concrete portion of the containment at any given pressure.

It is concluded that these objectives have been met. Procedures for evaluating the degree of cracking, the amount of deformations, the extent of yielding of the reinforcement and the rate of leakage associated with any given internal pressure as well as the ultimate pressure to cause fracture of the tendons were developed. These procedures were verified by the testing to failure of a 1/14 scale prestressed concrete containment structure in the laboratory. Excellent agreement was obtained between the predicted and observed behavior of this test structure. The leakage rates were not verified in this test. Details of the analytical procedures and the experimental results are contained in References 1 to 18. The main features of this work, and additional details of a crack and leakage computation technique, are summarized in this report.

Since the investigation was to study the overall behavior of the structure, details such as temporary openings during construction, air locks and other penetrations which could affect locally the behavior of the structure were not considered.

1.2 Overview of Developed Methodology

The investigation, which continued over a period of approximately five years, consisted of both analytical and experimental studies. These studies were interactive. That is, in order to develop the methodology to predict inelastic behavior of prestressed concrete containments, the results from one stage of the investigation were required either as input or for evaluation of other stages. This is demonstrated in the following summary.

The initial stage of the study dealt with elastic analyses of the G-2 containment structure (1). These analyses were carried out using the BOSOR4 Computer Code (22). During this stage a very simple computer code based on classical shell theory was developed (2). This program was intended for preliminary design and checking purposes and proved very useful in the design of the containment model.

While elastic analyses give a good indication of the condition of the structure prior to cracking, the behavior of the structure after cracking can be predicted only from a full nonlinear analysis. The remainder of the project was devoted to developing a technology that could give reliable results for post-cracking response of containment structures from the time of crack initiation until ultimate failure.

Since the maximum pressure that could be developed within the containment is dependent on the nature of the failures that occur in the safety systems, including the containment itself, the analyses were carried out assuming it was possible to develop the pressure necessary to develop the full capacity of the

structure. If a containment pressurized with a compressible fluid were leak-tight at the time the ultimate capacity was reached, the resulting failure would be explosive and probably disastrous. This aspect of containment behavior was discussed in References 3 and 13.

Obviously, however, an unlined containment structure strained to its maximum load carrying capacity would be extensively cracked and, therefore, would not be leak-tight. The real response of the structure to internal pressurization is then a rate-dependent problem. The maximum pressure that can be developed internally is reached when the rate of leakage from the building is equal to the rate of delivery of the pressurizing medium to the building. Although a detailed interactive analysis was outside the scope of this investigation, some basic data for such an analysis was obtained. One aspect of the investigation was, therefore, to obtain as accurate an estimate as possible of the cracking to be expected in the structure at various load levels. In order to obtain accurate estimates of cracking it is necessary that the analysis properly predict strains. This required the development of a technology to predict post-cracking strains in prestressed concrete thin shell structures, since no satisfactory technology was available at the initiation of the project.

In view of the preceeding considerations the following strategy was adopted. An analytical technique was developed to predict average strains in cracked prestressed concrete membrane elements (4, 11, 12). The necessary material properties were

deduced from laboratory tests of approximately 1/4 scale "wall segment" elements similar to portions of the wall of a typical containment structure (7). The analytical material model was then refined to the extent that the best correlation possible was obtained for the various types of specimens (5, 14, 15).

The analytical technique was then applied to a model containment structure which was tested to failure in the laboratory (4, 9, 17). The test structure was approximately 1/14 the size of a Gentilly-2 containment structure and, although it was not a scale model of this structure, had components modelled to simulate similar behavior. The correlation between the strains predicted by the analytical technique and those measured on the test structure established the validity of the technique as a valid tool to assess the behavior of the Gentilly-2 containment.

In addition to assessing the state of stress and strain within the structure for arbitrary internal pressures, an attempt was made to estimate leakage using the following methodology. Crack widths and spacings were measured on all wall segment tests and a correlation of this crack geometry with measured strains was inferred (8). Leakage through similar specimens was measured and related to the crack geometry (6). Based on the strains obtained from an analysis of the G2 structure, the crack geometry-strain relationship was then used to estimate the cracking in the G2 structure and the leakage relationship was used to estimate the leakage of this structure at various internal pressures (10).

While it is apparent that there is an intimate interaction

between the analytical development and the testing phases of the project, it should be pointed out that the testing phases of the project could be regarded as independent of any analytical development. The observation of the behavior of the test structure alone has provided valuable insight about the behavior of a containment structure without any analysis. However, the integration of the two phases of the project enhanced the interpretation of the results from each phase.

1.3 Scope of Report

The various stages of the methodology described in Section 1.2 are considered in more detail in the rest of this report. In each chapter one item needed to predict the behavior of a prototype containment is presented. Chapter 2 reviews the analyses developed to predict the strains, stresses and deformations in reinforced and prestressed containment structures. Chapter 3 presents the results of the wall segment tests and relates crack spacing and crack width to average strain. Several aspects of the behavior of the test structure are reviewed in Chapter 4, both to show the agreement between analysis and test and to show those areas where discontinuities such as the buttresses affected the behavior. Leakage of air through cracked concrete is discussed in Chapter 5 which concludes with an estimate of a pressure-leakage relationship for the concrete segments of the G2 containment.

1.4 Acknowledgements

The study was sponsored by the Atomic Energy Control Board of Canada and was under the general supervision of Dr. W. D. Smythe and Dr. F. Campbell. Principal investigators at the University of Alberta, Department of Civil Engineering, were Drs. J.G. MacGregor, D.W. Murray and S.H. Simmonds. Initially, Mr. Declan Whelan served as technical liaison between AECB and the project directors, however, from the summer of 1977, Dr. G.J.K. Asmis served in this capacity.

The progress of the project was reviewed from time to time by an Advisory Committee with representatives from the Atomic Energy Control Board, Atomic Energy of Canada Limited, Canatom Limited, Hydro Quebec and Ontario Hydro. The project directors wish to thank the members of this committee for the help and guidance received during this work.

Analytical studies were performed using the facilities of the Computing Centre, University of Alberta. Much of the computer work was done by Dr. M. Epstein, Dr. L. Chitnuyanondh and Mr. C. Wong. Testing was carried out at the I.F. Morrison Structural Laboratory at the University of Alberta. Dr. S.H. Rizkalla was in charge of laboratory work. Much of the data was reduced by Dr. L. Chitnuyanondh, Dr. M. El Zanaty and Mr. C. Wong.

The prestressing of the test structure was carried out by Con-Force Products Ltd. at no cost to the project. The authors sincerely appreciate the interest, guidance and help given by Con-Force at various stages of the project.

2. PREDICTION OF STRUCTURAL RESPONSE

Structural analyses of containment structures are carried out to determine the response of the structure to various types of loadings. These analyses produce estimates of the deformations, average strains and stresses. In this study the leakage is expressed as a function of the crack geometry which, in turn, is expressed as a function of the average strains. As a result, much of the following discussion concerns the calculation of strains in a reinforced or prestressed concrete structure.

2.1 Elastic Analyses

The initial stage of the study dealt with elastic analyses of the G-2 structure (1). The effects of gravity loads, prestressing loads, shrinkage, temperature, internal pressure, and construction sequence were included. It was shown that, for the structure under consideration, the effects of creep, shrinkage and construction sequence were small. Although the thermal effect could have a significant influence on cracking conditions, it had little influence on ultimate load capacity. The analysis was carried out using the BOSOR4 computer code (22).

During the initial stage of the project, it was also demonstrated that a very simple computer code based on classical shell theory (2) could be constructed which, except for some specific effects, yields results that are similar to those of BOSOR4 and are adequate for preliminary design and checking purposes. The deficiencies of this classical analysis are: (a) the effects of tapered thicknesses of shell elements on the

distribution of stress resultants cannot be included, and (b) short segments of spherical shells cannot be properly handled. In addition, the stiffening effect of the reinforcing steel is difficult to include. Unreported finite element studies confirmed the adequacy of these elastic analyses within the limitations of the elastic assumptions. The classical shell analysis proved very useful in the design of the model containment structure built and tested in the laboratory.

While elastic analyses give a good indication of the condition of the structure prior to cracking, their extrapolation to post-cracking conditions cannot provide accurate information on subsequent limit states. Estimates of these limit states were made on the basis of such extrapolations using simple strength design concepts. For these estimates it was necessary to assume that post-cracking stress resultants and/or deformations were proportional to their precracking values. The estimates were carried out with quasi-uniaxial assumptions and with more complex biaxial assumptions (11), but no assurances could be given that the results were reliable. The actual behavior of the structure can be predicted only from a full nonlinear analysis.

The remainder of the project was devoted to developing a technology that could give reliable results for the post-cracking response of containment structures, from the time of crack initiation until ultimate failure.

2.2 Prediction of Average Strains -- Inelastic Analyses

Average strains for prestressed concrete sections containing

layers of conventional steel reinforcement and loaded in biaxial tension were obtained into the postcracking region using a computer program (4, 11, 12) developed by modifying the BOSOR5 program (23). This program considers the structure as a series of axisymmetric shell segments which are defined with respect to a reference surface. The shell equations are solved using the finite difference energy technique assuming plane sections remain plane throughout the structure.

The shell segments are layered to represent the different materials encountered through the thickness of the segment. Material properties can be assigned uniquely to each layer as described in Reference 4. Each layer of reinforcement or prestressing steel is modelled as a separate layer with a thickness equal to that necessary to provide the same area per unit width as provided by the bars or cables. Bar cut-offs are modelled by tapering the bar linearly from full area to zero over the development length.

Mesh points are assigned to any location on the reference surface at which output of displacements, stresses and strains is desired. Mesh points are also required at any point where there is an abrupt change in the thickness of the section or of a layer, or where there is a change in loading conditions. Intermediate mesh points between the above control points are selected by the analyst such that, in his judgement, the model will be able to adequately represent the variation of stresses and strains. Hence mesh points are generally more closely spaced near the ends of structural components where the restraints

imposed by adjacent components may induce bending in addition to the membrane forces.

Loadings are simulated by distributed pressures applied to the reference surface, or by concentrated load acting at mesh points. Prestressing loads were simulated as distributed pressures except for anchorage forces and circumferential cable forces in the ring beam which were simulated as concentrated forces (4, 10).

The numbers of shell segments, mesh points and material layers used in the analysis of the Gentilly-2 secondary containment structure are given in Fig 2.1. Material properties were assigned to the different layers individually.

For concrete layers in tension the affect of tensile stiffening of the concrete between cracks in the post-cracking region was modelled using a degrading stress strain curve as shown in Fig 2.2. These properties were obtained from correlations with laboratory tests on wall segments having similar reinforcing and loading conditions (8) to those in the prototype structure (4, 7, 14).

The strains computed in this manner are average strains, ε_m, in that the total deformations even in the post-cracking region are considered to be "smeared" uniformly over the length. This is in contrast to the real behavior where large strains occur at cracks and smaller strains between the cracks. Hence, although the total deformations computed from these strains are representative of the response of the entire section to overpressure loading up to failure, they do not indicate directly

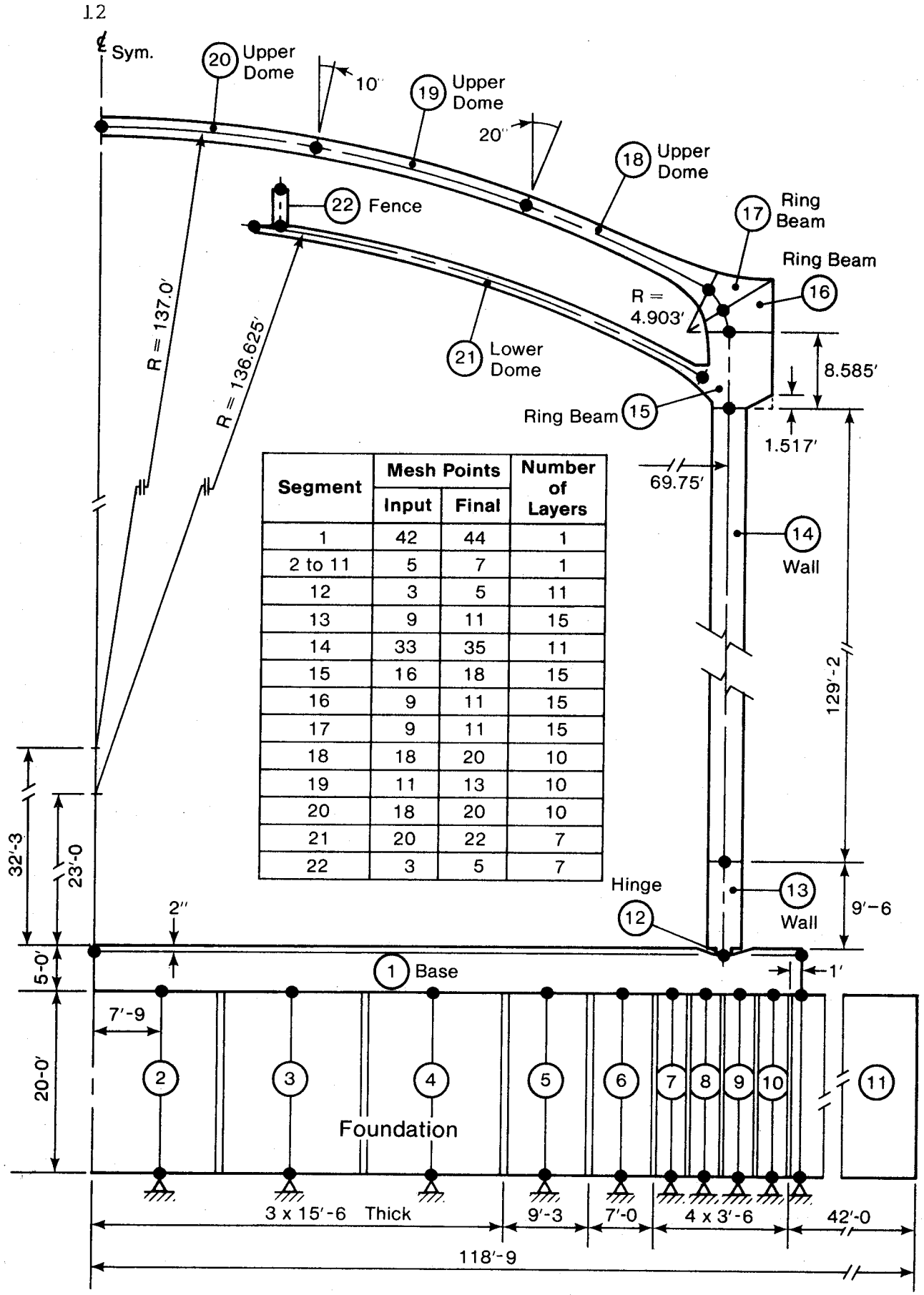

Segment	Mesh Points		Number of Layers
	Input	Final	
1	42	44	1
2 to 11	5	7	1
12	3	5	11
13	9	11	15
14	33	35	11
15	16	18	15
16	9	11	15
17	9	11	15
18	18	20	10
19	11	13	10
20	18	20	10
21	20	22	7
22	3	5	7

Figure 2.1 BOSOR5 Model of Gentilly E Containment - Segment Identification

Point	Strain	Stress (psf)
1	0.0	0.0
2	0.0000142	8,244
3	0.00012	18,320
4	0.00030	17,400
5	0.0015	10,050
6	0.0028	5,491
7	0.0039	3,924
8	0.2000	2,000

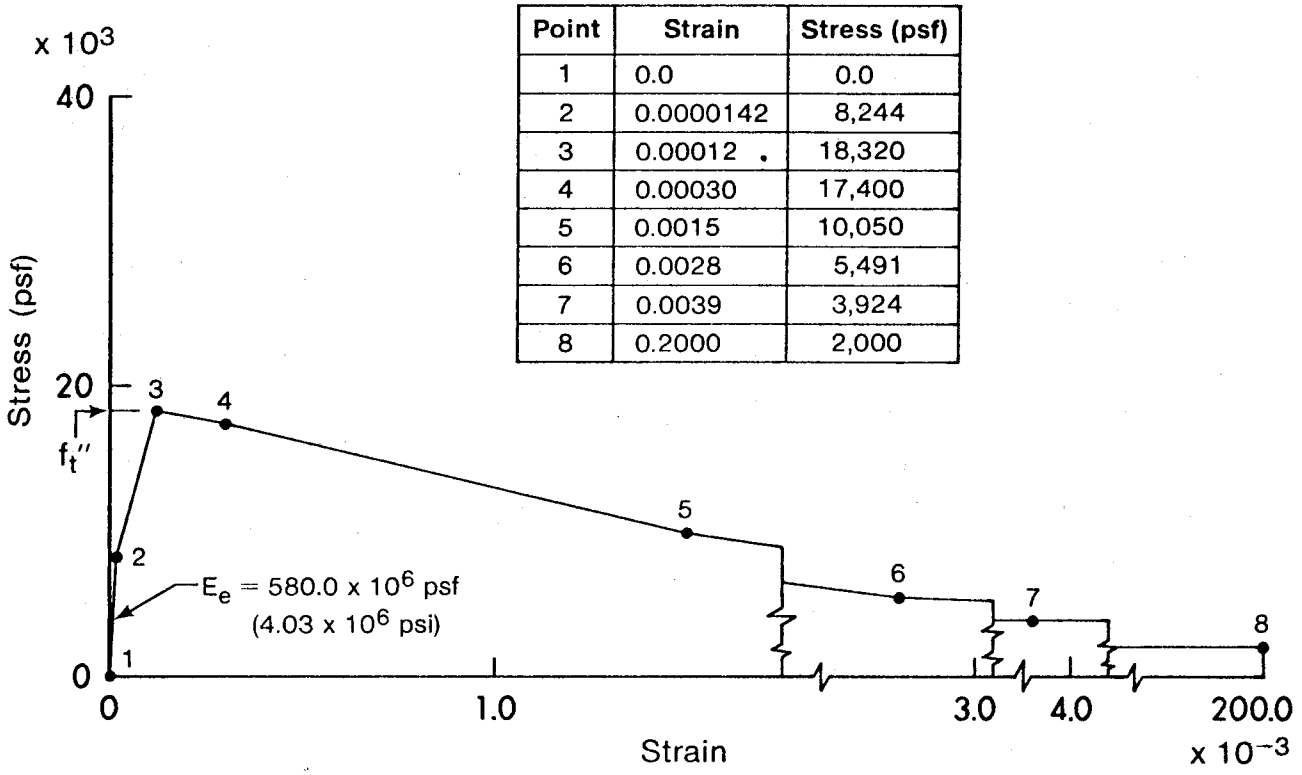

Figure 2.2 Tensile Stress-Strain Relationship for Reinforced Concrete

the spacing or width of cracks that result from these strains. A means of predicting the corresponding cracking and a description of the segment tests on which the procedure is based is contained in Chapter 3 of this report.

Strains computed using the modified BOSOR5 technique just described, corresponded closely with average strains measured in the test structure (9) except in the immediate vicinity of the buttresses. Since the analytical modelling of the structure and loading is axisymmetric, the stiffening effects of the buttresses were not included in the analysis. The observed behavior in the region of the buttresses is discussed in Chapter 5 of this report. On the basis of these comparisons it may be concluded that the modified BOSOR5 computer code developed in this study is entirely adequate to estimate the high overload response of containment structures of the Gentilly-2 type.

3. CRACKING OF PRESTRESSED CONCRETE SECTIONS

The computed average strains agree closely with measured strains obtained by measuring the elongation over a length that includes several cracks. The next step in the methodology developed in the study is to predict the spacing and width of cracks corresponding to these average strains. Since this is dependent on the reinforcing and prestressing details of the section and must be based on empirical studies, a short description of the wall segment tests used to "tune" the analysis and develop the procedure for crack prediction is required.

3.1 Wall Segment Tests

To determine the response of prestressed concrete sections to tensile forces a total of twelve 1/4 scale wall segments designed and loaded to represent various locations in a containment structure were constructed and tested to failure (7). A typical segment was 31.5 in. square by 10.5 in. thick, reinforced in two directions and prestressed in one or two directions as shown in Fig 3.1. Major variables were the ratio of prestressing in the two directions, variations in concrete cover and bar spacing, combined axial tension and moment, scale effects, and lap splices of reinforcement. The variables for each segment are summarized in Table 3.1.

Loads were applied to the segments by pulling on the reinforcement and prestressing strands using specially designed loading yokes to ensure uniform strain over the section, see Fig 3.2. Circumferential loads were applied using a 1,400,000 lb.

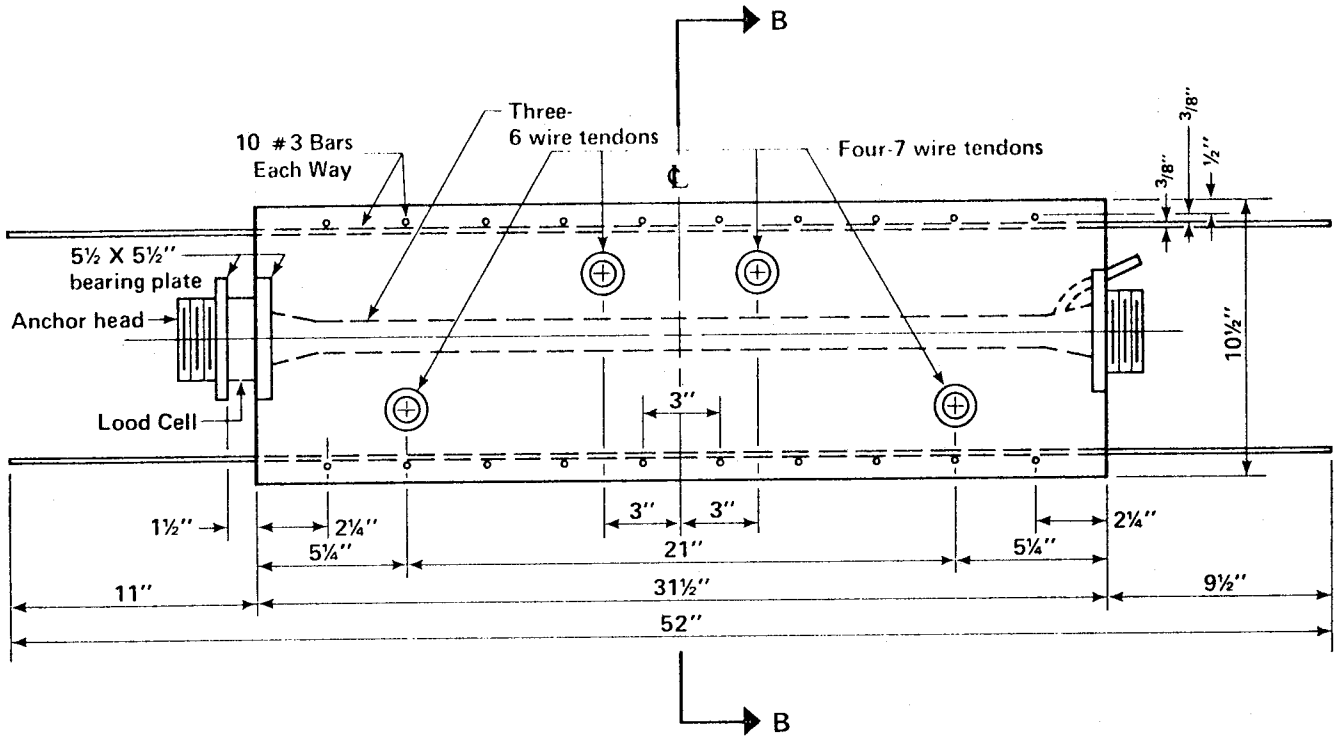

(a) Section A-A

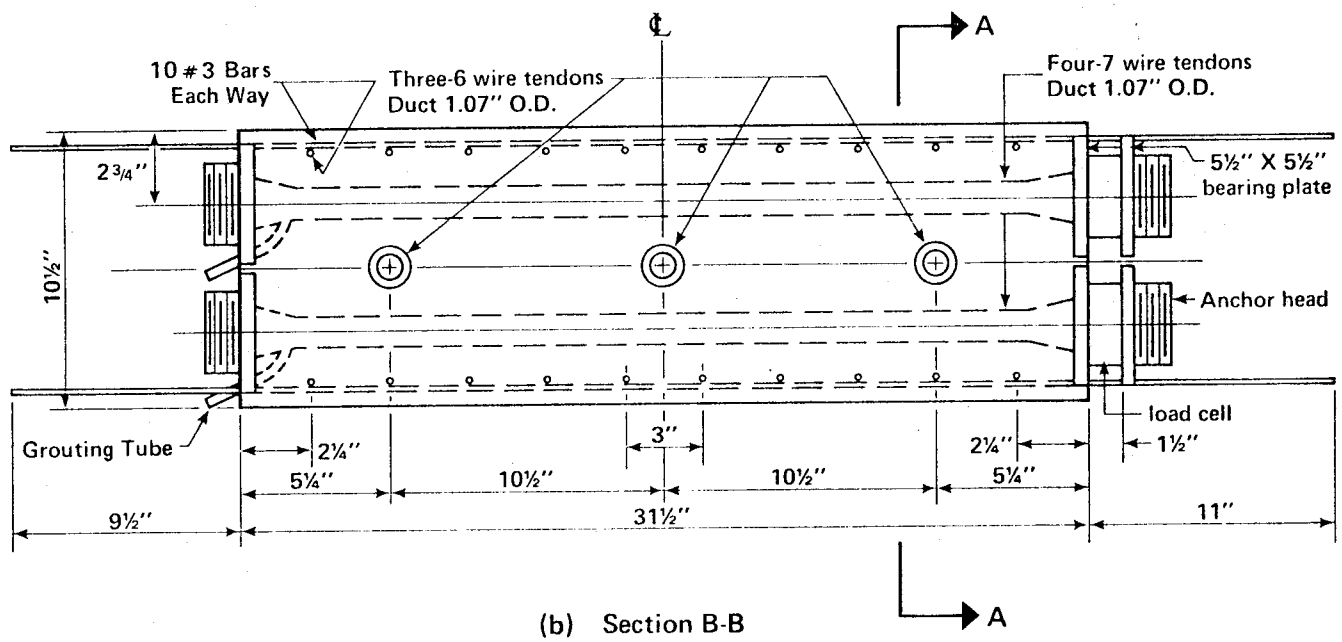

(b) Section B-B

Figure 3.1 Sections Through Wall Segment Specimen

Table 3.1 - Overview of Variables Considered in Wall Segment Tests

Specimen	Prestressed	Non-Prestressed Reinforcement per Layer, 1**	Min. Concrete Cover in.	Loading Ratio H/V	Thickness in.	Special Features
1	two	10 #3 @ 3 in.	0.5	1:2	10.5	
2	two	10 #3 @ 3 in.	0.5	1:2	10.5	
3	two	10 #3 @ 3 in.	0.5	1:1	10.5	
4	none	8 #4 @ 4 in.	0.5	1:1	10.5	
5	one***	10 #3 @ 3 in.	0.5	1:0	10.5	
6	one***	8 #4 @ 4 in.	0.5	1:0	10.5	
7	none	6 #6 @ 6 in.	0.75	1:1	15.75	
8	two	10 #3 @ 3 in.	1.25	1:2	10.5	
9	two	10 #3 @ 3 in.	0.5	1:2	10.5	Lap Splices
10*	two	10 #3 @ 3 in.	0.5	1:2	10.5	Leakage Test
11	two	10 #3 @ 3 in.	0.5	1:2	10.5	Lap Splices
12	two	10 #3 @ 3 in.	0.5	1:2	10.5	Applied Moment
13	two	10 #3 @ 3 in.	0.5	1:2	10.5	Applied Moment
14*	one	10 #3 @ 3 in.	0.5	1:0	10.5	Leakage Test

* These tests involve air leakage measurements.

** Each face of the specimen had one such layer in each direction.

*** Three tendon direction only, other tendons omitted.

capacity MTS testing machine and "longitudinal" loads were applied by four 200 kip capacity hydraulic rams reacting against a load frame designed for the tests.

Approximately 160 measurements were recorded at each load level and included such items as vertical load, horizontal load, forces transferred to tendons, forces transferred to reinforcement, reinforcement strains, concrete strains, elongation of specimen, crack widths, and slip of tendons. A typical test of a wall segment took approximately 6 days to set up and initialize, one day to run, and one day to dismantle. Loading was applied in increments and terminated at approximately 95% of the rupture strength of the tendons to avoid damage to loading apparatus and instrumentation.

3.2 Determination of Crack Spacing

A comprehensive survey of existing procedures for predicting crack spacing and widths was made and reported in Reference 8. The application of these techniques did not predict the observed crack spacing and size observed with the wall segments. This was not entirely unexpected since none of the previous investigators had considered prestressed sections with such large amounts of reinforcing and loaded in biaxial tension. This necessitated the development of a means of predicting the spacing and size of cracks from computed mean strains that was applicable to containment type structures.

It was observed in the segment tests that, when a load was applied, the specimens initially cracked at one location. With

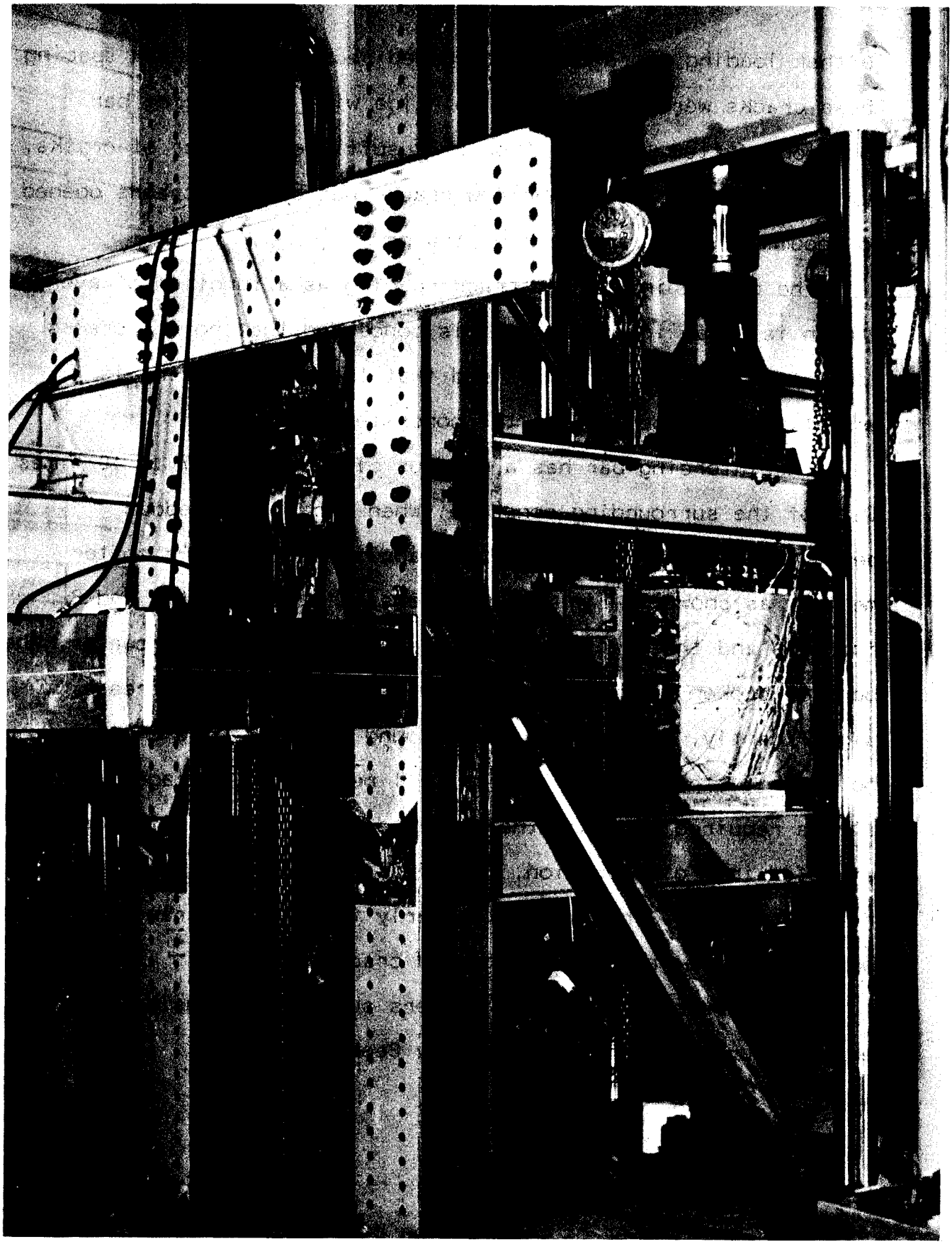

Figure 3.2 Loading Frames for Segment Tests

further loading, more cracks occurred reducing the crack spacing. These cracks were observed to coincide with reinforcing bar locations. After the formation of a sufficient number of cracks, further loading produced no new cracks but certain cracks opened to accommodate the increasing strains.

The change in average crack spacing as a function of average strain is given in Fig 3.3. It is concluded that no new cracks form after a strain of 0.002 and that the crack spacing is essentially independent of the concrete cover.

A reinforcing bar has a modulus of elasticity 7 to 10 times that of the surrounding concrete. When a bar is embedded perpendicular to the direction of applied stress in a softer medium, as shown in Fig 3.4, the tensile stresses at A and B increase and those at C and D decrease slightly. If, however, the bond is broken at A and B, the stresses at C and D increase significantly, approaching those found adjacent to a circular hole. This stress concentration will reduce the average tensile stress required to crack the concrete. As a result, if a crack is expected in a given region, it will likely occur at a transverse reinforcing bar. This is particularly true if the transverse bar spacing is similar to the expected crack spacing.

For reinforced concrete members subject to tension, the expected crack spacing is given by Beeby (24) as

where

$$s = 1.33c + 0.008d_b \, A/A_b \qquad (3.1)$$

c = concrete cover

d_b = diameter of reinforcing bar

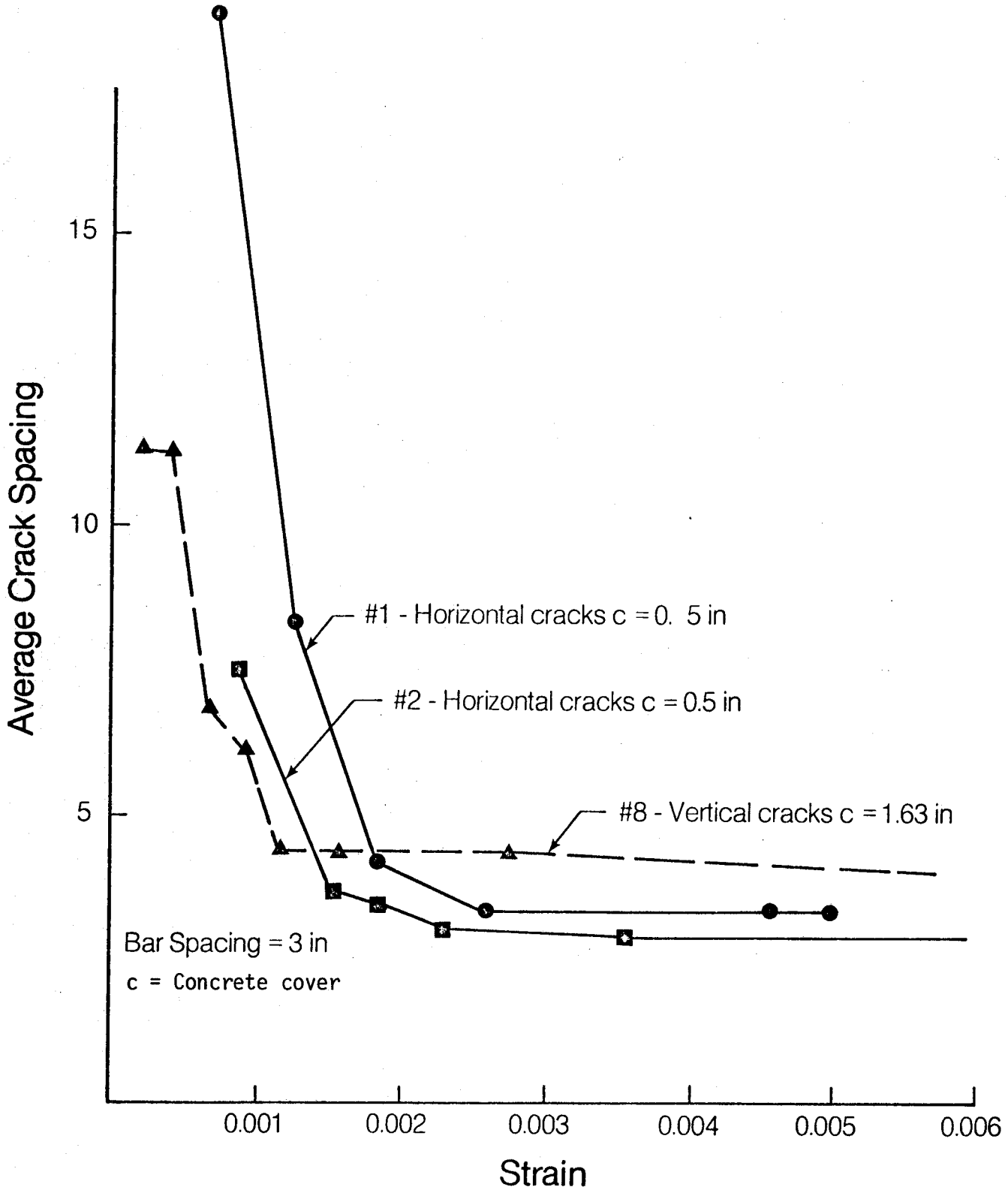

Figure 3.3 Effect of Cover, Bar Spacing and Strain on Crack Spacing

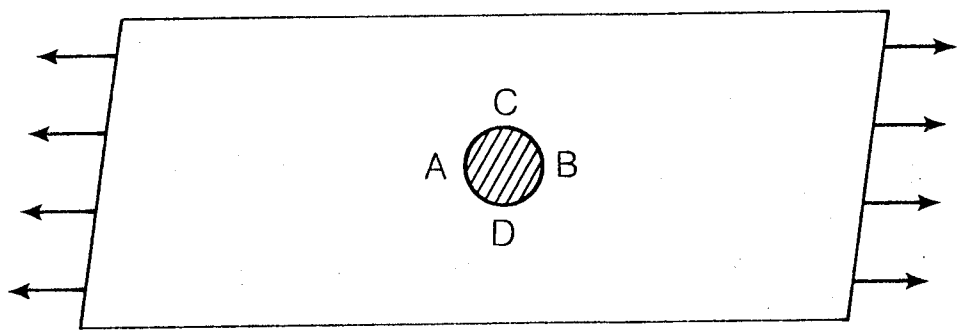

Figure 3.4 Bar Embedded in Concrete

A_b = area of reinforcing bar

A = area of concrete concentric to the bar

If the spacing of the reinforcing bars is between a half and one times the minimum expected crack spacing the stress concentrations at the bars should be enough to cause cracking at each bar location. For bar spacings between one and two times the minimum expected spacings, the formation of cracks along the bars should make additional cracks between bars unlikely. Thus surface cracks should be expected to follow transverse bars if these bars are spaced between half and two times the expected crack spacing. Such cracking was typical of that observed in the segments, see Fig 3.5.

To determine how the cracks propagated through the wall a number of specimens were sawn in two. The cracking patterns within Segment 1 and Segment 2 are shown in Fig 3.6. The cracks in Segments 1 and 2 respectively, in Fig 3.6 are representative of meridional and circumferential cracks expected in the prototype. From an examination of all the segments it was concluded that roughly one-half of the cracks extended through the segments and in most cases these cracks divided near the surface to form two surface cracks. In all wall segments which had prestressing tendons parallel to the cracks, the through-the-wall cracks occurred at the prestressing tendons. In these cases, surface cracks which did not penetrate through the wall developed at strains greater than about 80% in the yield strain of the reinforcing bars.

From further observations of the segments, it was concluded

(a) Face A

(b) Face B

Figure 3.5 Cracks in Segment 2 at End of Test

(a) Horizontal Cracks in Segment 1 (Face A Upwards)

(b) Vertical Cracks in Segment 2 (Face A Upwards)

Figure 3.6 Sections through Segments 1 and 2 at Ends of Tests

that the effects on cracking of the transverse state of stress in segments loaded in biaxial tension were small and could be ignored in crack width calculations with relatively little error; the presence of bar splices did not significantly affect crack widths for average strains up to 0.002, although at high strains the existing cracks at the ends of the splice tended to open more; and, while the presence of bending moment had a predictable effect on surface strains and hence cracking, the presence of moment about one axis had little effect on the widths of cracks perpendicular to that axis.

As a result of these observations, a series of rules were developed for use in computing the mean spacing of cracks in the wall segment specimens. It is expected that the same rules would apply in the prototype structure.

1. If the spacing of transverse bars is between 0.5 and 2 times the crack spacing computed from Eq. 3.1, cracks will form along each of the transverse bars by the end of the test. The cracking will be limited to these cracks.
2. The spacing of cracks at the surface of the speciment is independent of the radial distance from the longitudinal bars (bars perpendicular to the cracks) to the point on the surface where the cracks are observed.
3. In walls containing prestressing tendons parallel to the direction of cracking, through-the-wall cracks will occur at the same spacing as the tendons. Should the tendon spacing exceed twice the wall thickness an additional through-the-wall crack will occur midway between the tendons.

4. In walls without prestressing tendons parallel to the direction of cracking, through-the-wall cracks will occur at every second reinforcing bar and not further apart than the wall thickness.
5. The number of through-the-wall cracks will stabilize by the time the strain reaches 0.002. At any given strain less than 0.002 the number of through-the-wall cracks can be given as:

$$N = N_{twc} \left(\frac{\varepsilon_{s2} - \varepsilon_{s2,cr}}{0.002 - \varepsilon_{s2,cr}} \right) \qquad (3.2)$$

where N is the number of through the wall cracks at the load in question: N_{twc} is the final number of through-the-wall cracks according to assumptions 3 or 4; ε_{s2} is the strain in the reinforcing bars at the crack (See Eqn. 3.6); $\varepsilon_{s2,cr}$ is the average strain at the onset of cracking (See Eq. 3.10).

6. At a strain of 0.002, surface cracks form so that the final spacing agrees with rules 1 and 2.

3.3 Computed Mean Crack Width

When computing crack widths it is necessary to distinguish between through-the-wall cracks which result in paths of leakage and surface cracks which do not. In leakage calculations it is sufficient to consider only through-the-wall cracks while for comparison to cracking tests the widths of both types must be included. Also, although there will be a statistical distribution

of crack widths only computations for the representative or mean width is considered here since in a structure as large as a containment vessel the leakage can be expressed as a function of the average crack width.

The procedure outlined below may be used to determine crack widths and spacings for prestressed wall sections containing two layers of reinforcement near each face in percentages and spacings normally associated with secondary containments. The procedure is based partly on a modification of a theory proposed by Leonhardt (25) and partly on the observations listed in Section 3.2.

The width of through-the-wall cracks is computed first since surface cracks that do not penetrate through the wall are assumed to occur to relieve tension build up in the concrete between the through-the-wall cracks and will generally not form until the reinforcing bars have yielded at the through-the-wall cracks. The expected spacings of these cracks was presented in Section 3.2.

The width of a through-the-wall crack computed at the tendon is assumed to be divided evenly between two cracks extending to the surface given by the equation:

$$w_{twc} = \varepsilon_{s2}\ell_o + \varepsilon_m\ell_t \qquad (3.3)$$

where:

ε_{s2} = steel strain at the crack, Eq. 3.6

ℓ_o = unbonded length at a crack, Eq. 3.11

ε_m = average strain measured over a length that includes

several cracks, Eq. 3.8, or the mean strain from the analysis described in Section 2.2.

ℓ_t = bond transfer length, Eq. 3.4

The bond transfer length, ℓ_t , was taken as

$$\ell_t = s - \ell_o \tag{3.4}$$

At any load level subsequent to critical cracking but prior to yielding the reinforcing bars the steel stress and strain is given by:

$$f_{s2} = \frac{P - F_{se}}{A_s + A_p} \tag{3.5}$$

and $$\varepsilon_{s2} = f_{s2}/E_s \tag{3.6}$$

where

F_{se} = effective prestress force after losses

A_s = area of reinforcing bars

A_p = area of prestressing tendons

E_s = modulus of elasticity of steel

When the force P exceeds that required to yield the reinforcing bars the value of f_{s2} should be taken as f_{p2} where:

$$f_{p2} = \frac{P - A_s f_y}{A_p} \tag{3.7}$$

and the value of ε_{se} can then be obtained from the stress-strain curve for the tendon.

The mean strain, ε_m , is computed as:

$$\varepsilon_m = \varepsilon_{s2}\left[1 - \left(\frac{f_{s2,cr}}{f_{s2}}\right)^2\right] \tag{3.8}$$

These terms can be evaluated as follows. The average stress and strain in the reinforcement at the beginning or onset of cracking are defined as:

$$f_{s2,cr} = \frac{P_{cr} - F_{se}}{A_s + A_p} \tag{3.9}$$

and

$$\varepsilon_{s2,cr} = f_{s2,cr} / E_s \tag{3.10}$$

where

P_{cr} = the tensile force required to crack the section

The length of almost lost bond, ℓ_o, is obtained from the expression:

$$\ell_o = \frac{f_{s2,cr}}{6500} d_b \tag{3.11}$$

where ℓ_o is in units of psi and d_b is the diameter of reinforcement in inches. For a tendon, d_b taken as the diameter of an equivalent bar having the same cross-sectional area as the wires in the tendon.

Widths of surface cracks are computed in a similar manner from the expression:

$$w_s = \varepsilon_{se}\ell_{os} + \varepsilon_m \ell_{ts} \tag{3.12}$$

where ε_{s2} and ε_m are the same as for through-the-wall crack computations.

The effective unbonded length at a surface crack, ℓ_{os}, may be computed from:

$$\ell_{os} = \frac{f_{s,cr} d_b}{6500} \tag{3.13}$$

where:

$f_{s,cr}$ = $f'_t A/A_b$ (psi)

f'_t = tensile strength of concrete

A = area of concrete concentric to bar

= $(2c + d_b)$·(bar spacing)

c = concrete cover

A_b = area of a single reinforcing bar adjacent to the surface.

The bond transfer length at surface cracks, ℓ_{ts}, is taken as:

$$\ell_{ts} = \text{(bar spacing)} - \ell_{os} \qquad (3.14)$$

3.4 Comparison of Computed and Measured Crack Widths

While the widths of individual cracks and crack width distribution were determined for both the wall segments and the test structure (8, 9), only the mean crack or representative crack is required to predict overall behavior and leakage. An evaluation of the procedures developed in Sections 3.2 and 3.3 for determining the spacing and magnitude of the mean crack can be made by comparing the computed total elongation over a gage length, L, which contains several cracks, with the measured elongations over the same length. In computing this elongation the elastic elongation is neglected as being small when compared to that caused by cracking, hence the total elongation is assumed to be the sum of the crack widths or Σw.

Prior to yielding of the reinforcement the computed elongation is assumed equal to:

$$\Sigma w = N_{twc} \cdot w_{twc} \qquad (3.15)$$

where N_{twc} and w_{twc} are the number and mean width of the through-the-wall cracks in the assumed gage length. After yielding of the reinforcement the total elongation is:

$$\Sigma w = N_{twc} \bullet w_{twc} + N_s \bullet w_s$$

where N_s and w_s are the number and mean widths of the surface cracks.

Comparisons with measured data were on the basis of the dimensionless ratio, $\Sigma w/L$. In the range of loading from a strain of 0.0005 to 0.002, that is, for the period that cracks are growing and extending, for segment specimens without splices or moments (segments 1 to 6 and 8), the mean ratio of measured to computed $\Sigma w/L$ was 1.07 with a coefficient of variation of 0.347.

4. BEHAVIOR OF CONTAINMENT SUBJECTED TO OVERPRESSURE

To assess the reliability of the methodology to predict structural response at high internal pressures and to obtain some insight into the effects of the stiff buttresses and the modes of failure, a prestressed concrete containment structure was built and tested to failure in the laboratory. This test structure was patterned after the Gentilly-2 type secondary containment and was designed to behave and fail in a similar manner. Practical considerations in the construction and testing of the model meant that the same scale could not be used for all structural elements. As a result, while the overall behavior of the model would be similar to the prototype, there would not be a one to one correspondence of pressure at each limit state between the structure tested and the prototype containment. For this reason, the test structure should be viewed as a structure in its own right rather than as a model of a particular existing containment structure. The results from this test structure are contained in the following sections.

4.1 Description of the Test Structure

Since the test structure was designed to indicate behavior at high internal pressures, only those components of the prototype resisting internal pressure were included in the model. Hence the lower dome for the dousing system was not included in the model and the base was designed to be rigid rather than a slab on an elastic foundation. The connection between the base and the wall, however, was designed to act as a hinge in a manner

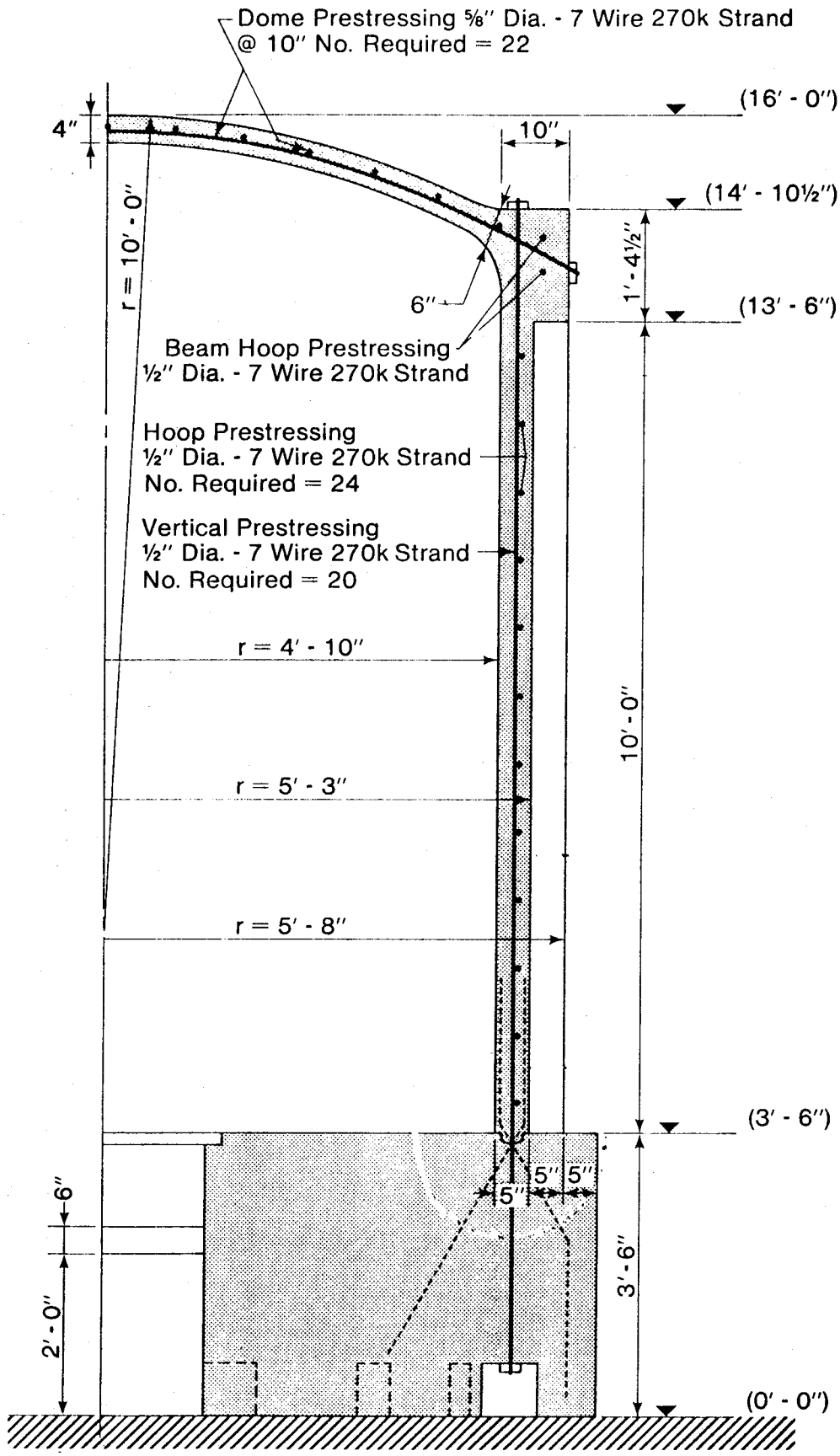

Figure 4.1 Vertical Section Through Test Structure

similar to the prototype.

The test structure had a height above the base of 12'-6" and an outer wall diameter of 10'-6" corresponding to an overall scale of 1:14 compared to the prototype. A vertical section through the test structure is shown in Fig 4.1 and a photograph of the completed structure after testing is shown in Fig 4.2. Complete details of the design criteria, material properties and construction techniques are given in Reference 9. Reinforcement and prestressing details resembled those of the prototype and were proportioned to give the same sequence of behavior as elastic analyses had predicted for the prototype.

In order to maintain a constant pressure while readings were being taken and to obtain sufficient internal pressure to cause failure, a flexible liner was used to prevent leakage. To prevent an explosive type failure the fluid used for loading was water.

Extensive measurements were made during loading of the test structure. Quantities measured electronically included internal pressure, deflections, steel and concrete strains, and those measured manually included concrete surface strain, crack widths and meridonal relations. Electronically read quantities were obtained from electric resistance strain gages and LVDT's (Linear Variable Differential Transformers) from which the voltage output was sampled and converted to digital form by various pieces of data logging equipment that were monitored and recorded using NOVA 210/E digital computer. In general, readings were taken electronically at pressure intervals of 5 psi and manual readings at intervals of 10 psi. A full description of the measuring

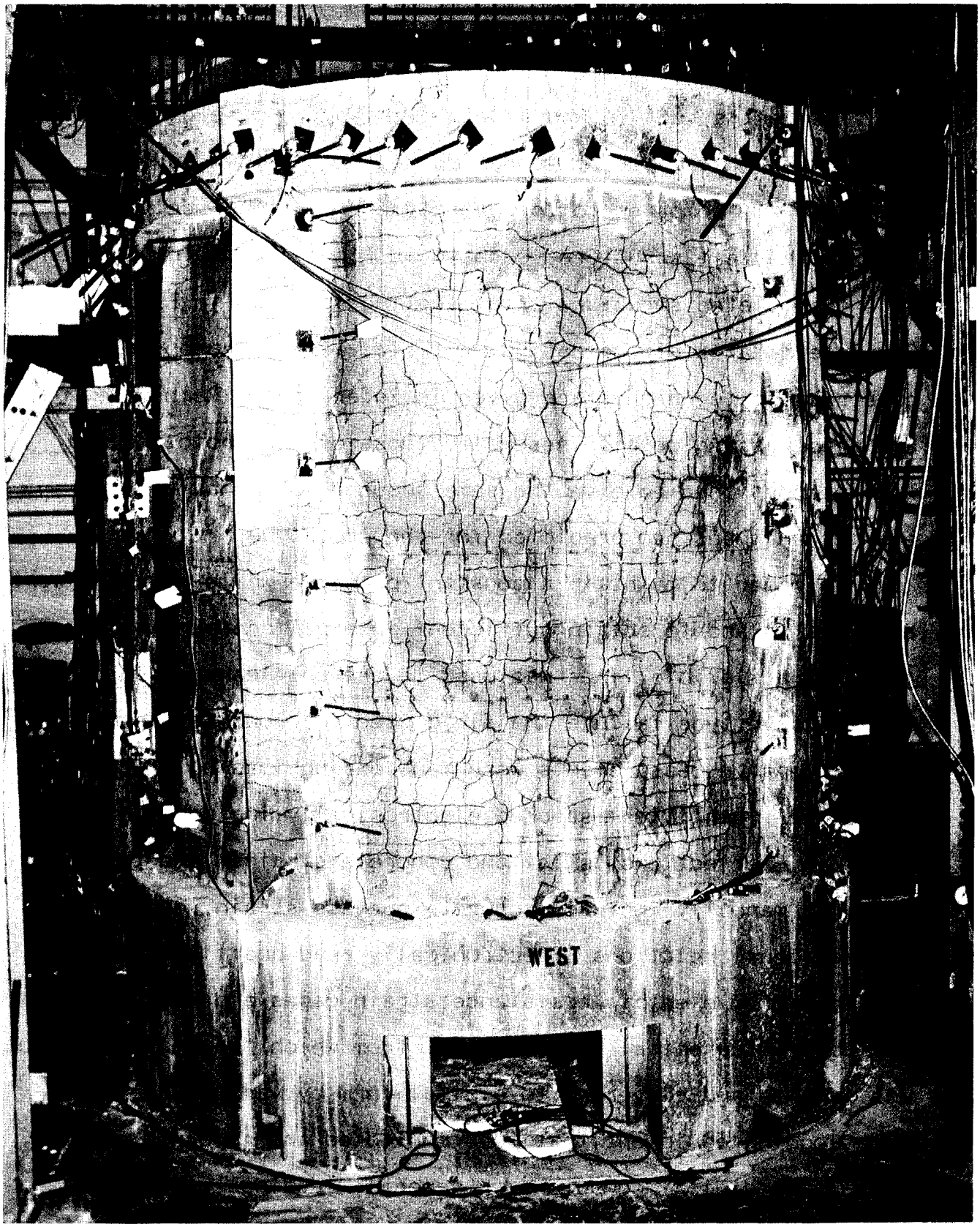

Figure 4.2 Photograph of Containment Structure After Test

devices, their location and the data acquisition system is given in Reference 9.

Zero internal pressure was defined as the condition with the model full of water and the top vent open to the atmosphere. Due to the weight of water there was a pressure gradient of 5 psi to the base of the wall. However, the zero readings for all gages are the values corresponding to zero pressure as defined above.

Seven separate tests (A to G) were conducted. The first five were all conducted at relatively low pressures below 40 psig and were used primarily to test the instrumentation and data processing systems. On the basis of these runs extensive modification to the instrumentation and access door gasket details were made.

The sixth test, Test F, was to have been the test to failure, however the test was stopped at 80 psig because of leakage of the liner and the difficulty in increasing and maintaining pressure. During this test extensive cracking of the structure was observed over much of the shell surface. For this reason, Test F was taken to represent the "virgin" response of the structure for cracking and results from this test have been included in the discussion of results in this chapter and in Chapter 3.

A new liner was fabricated and inserted inside the patched initial liner. The final test to failure, designated as Test G, took two days to complete. No leakage was observed during this test until the final failure pressure was reached.

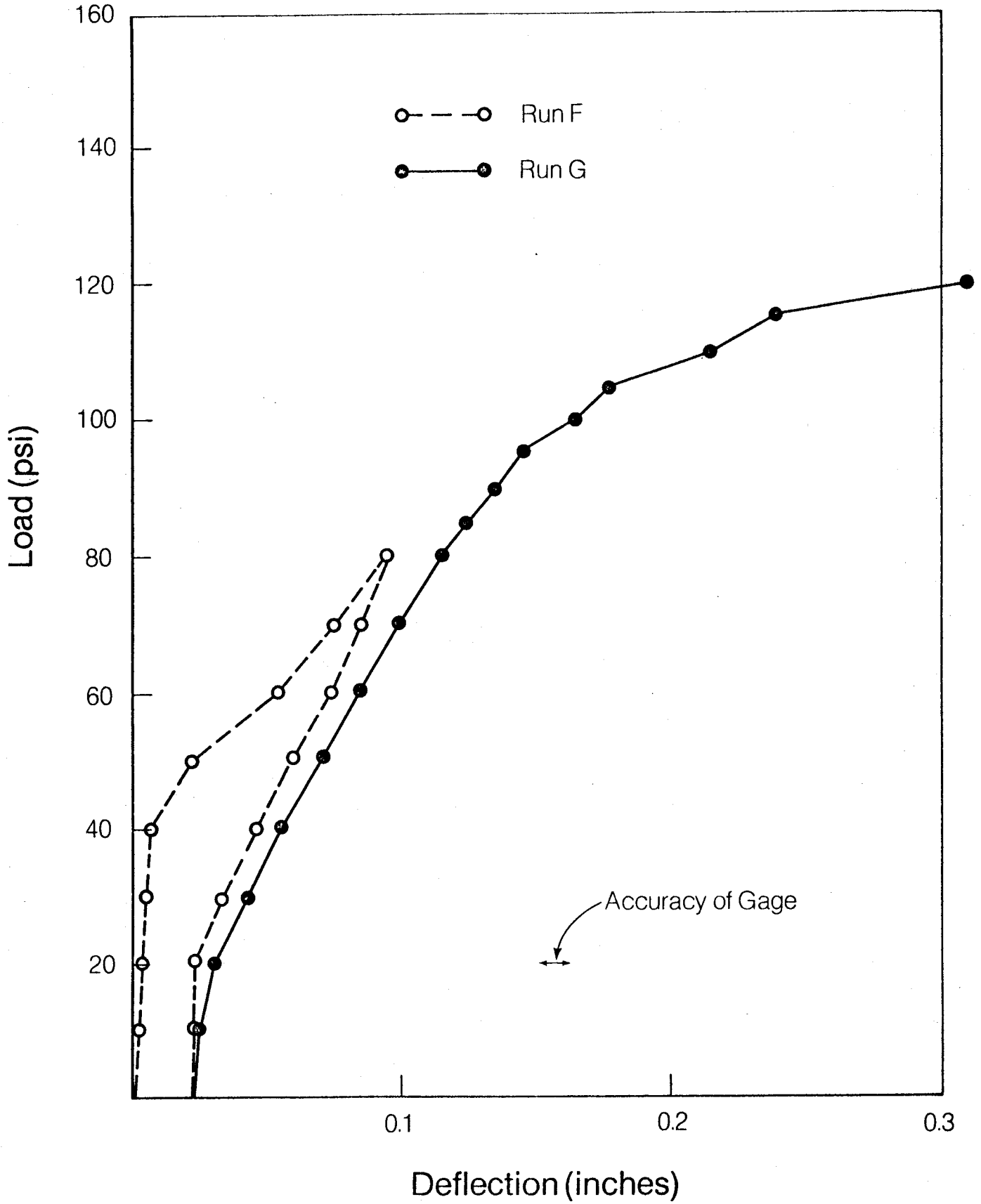

Figure 4.3 Pressure vs Horizontal Deflection of the Wall, 71.25 in. above Base

4.2 Observed Behavior of Test Structure

After the preliminary tests (A to E) the total residual deflections at midheight of the wall and crown of the dome were less than the specified accuracy of the LVDT's (0.015 in.). Thus it was assumed that the residual deflections at the start of Test F were negligible and were taken as zero. However, after the last load increment of Test E at 40 psi, two horizontal cracks were observed in the wall at 25 and 66 inches above the base. In addition two strain gages mounted on the inside surface of the concrete ceased to function at this pressure indicating they may have been crossed by a crack. Thus initial cracking occurred between 35 and 40 psi.

The response of the structure to increasing pressure may be obtained from load-deflection plots as given in Fig 4.3 and 4.4 (note the difference in the scales). These give the deflections at the midheight of the wall and at the crown of the dome, respectively. The reduced stiffness at the point of cracking in Test F is clearly indicated at between 40 and 50 psi. At both locations there was residual outward deflection after unloading.

At 80 psi, the maximum pressure reached in Test F, the crack pattern over the wall and dome was well developed and there was a strong correlation between the crack and tendon patterns. At higher loads, Test G, these cracks became wider and new cracks developed, again reflecting the tendon and reinforcement locations. The crack pattern for the dome at 80 psi is shown in Fig 4.5. This photograph show clearly the outer protion of the dome in which, due to the bending caused by the presence of the

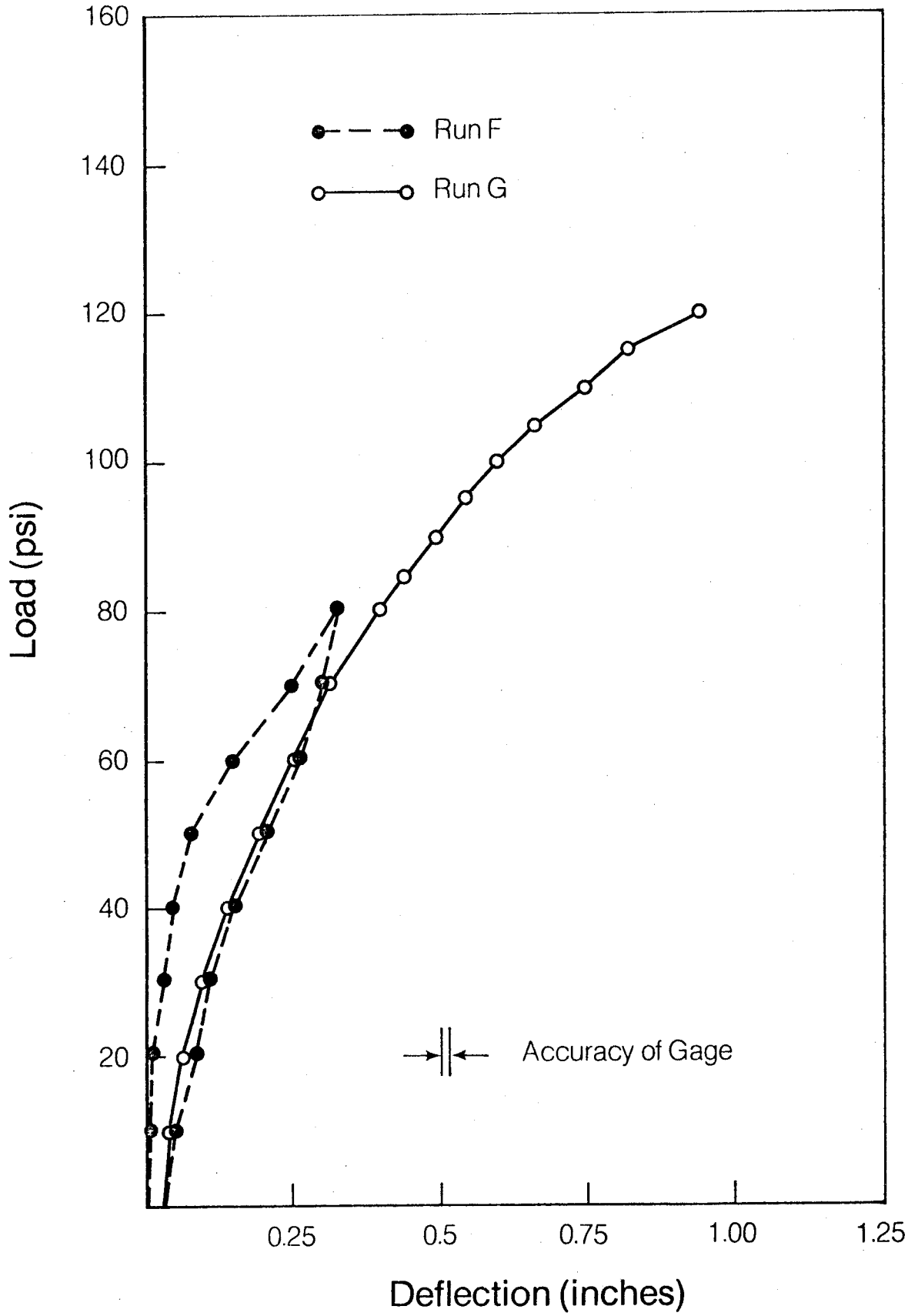

Figure 4.4 Pressure vs Vertical Deflection at Crown of Dome

Figure 4.5 Cracking in East Quadrant of Dome at End of Loading F, 80 psi

ring beam, there were no visible cracks throughout the test.

The crack pattern in the wall at 135 psi is shown in Fig 4.6. Attention is drawn to the horizontal cracking existing along the face of the buttress. Also visible is the outward bulging of both the wall and buttress. At pressures higher than this, an increase in pressure caused a considerable increase in deformations although no new cracks developed.

The ductility of the test structure at high pressures may be seen from the load-deflection plots in Fig 4.7 which are the full range of values for Test G for the two points given in Fig 4.3 and 4.4.

Due to the large increase in volume associated with the outward deformations it was difficult to increase pressure using the low volume hand pump. At a pressure of 149.5 psi the loading was terminated after 16 hours of continous testing. As a precaution, the load was reduced to 137 psi for overnight which accounts for the breaks in the curves at this pressure. When loading was resumed after an interval of 14 hours using a truck mounted high capacity pump, the pressure had dropped only 2 psi. The gap between the two points after reloading to the previous pressures is an indication of the creep that occurred during this period. Thus, although the test structure was cracked extensively and the internal pressure was over 85% of that to cause failure when it was left over night, the test structure was able to maintain this pressure with very little additional deformation. This was not altogether unexpected as the structure was essentially being held together by the prestressing tendons.

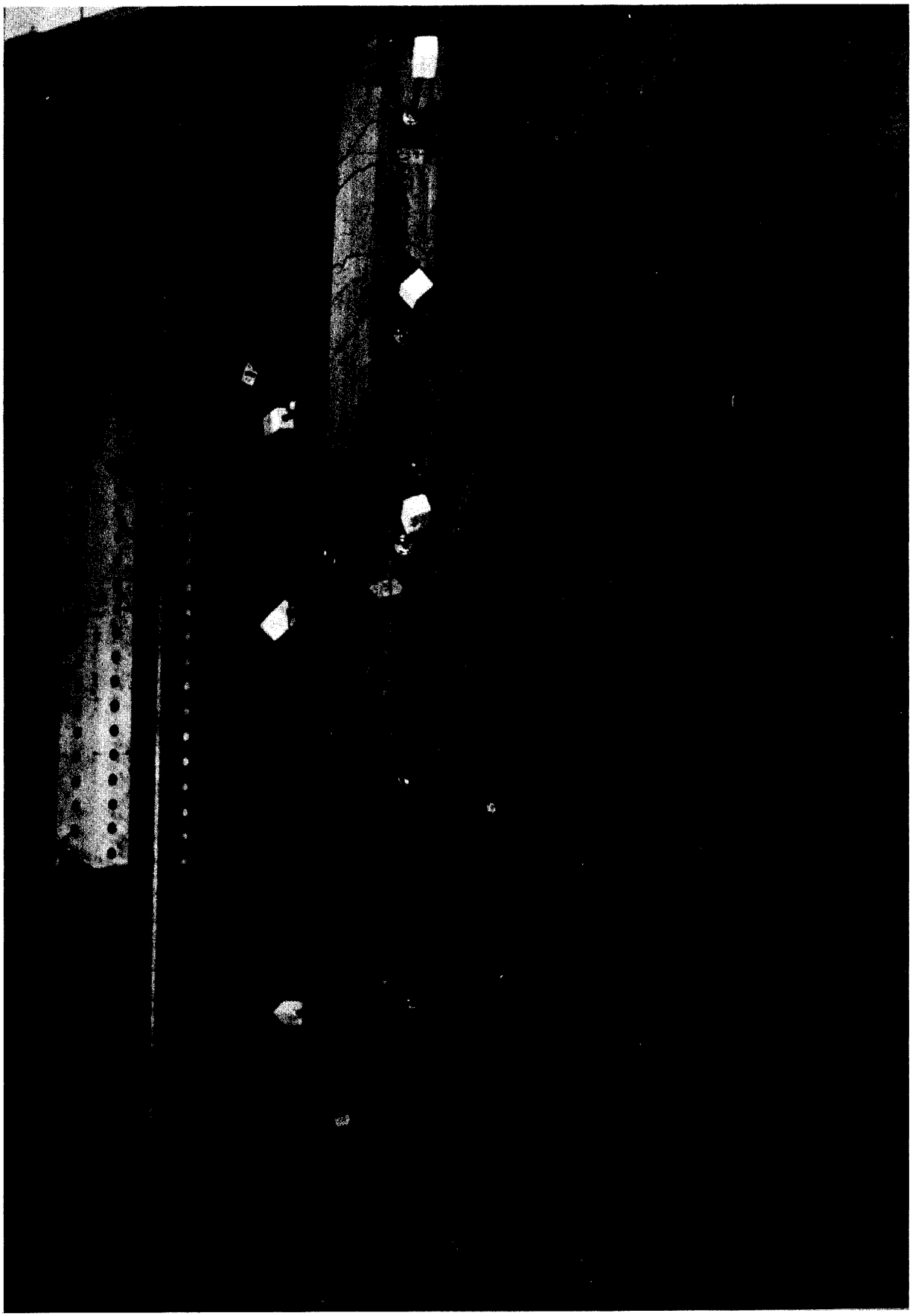

Figure 4.6 Outward Bulging of Northwest Buttress at 135 psi

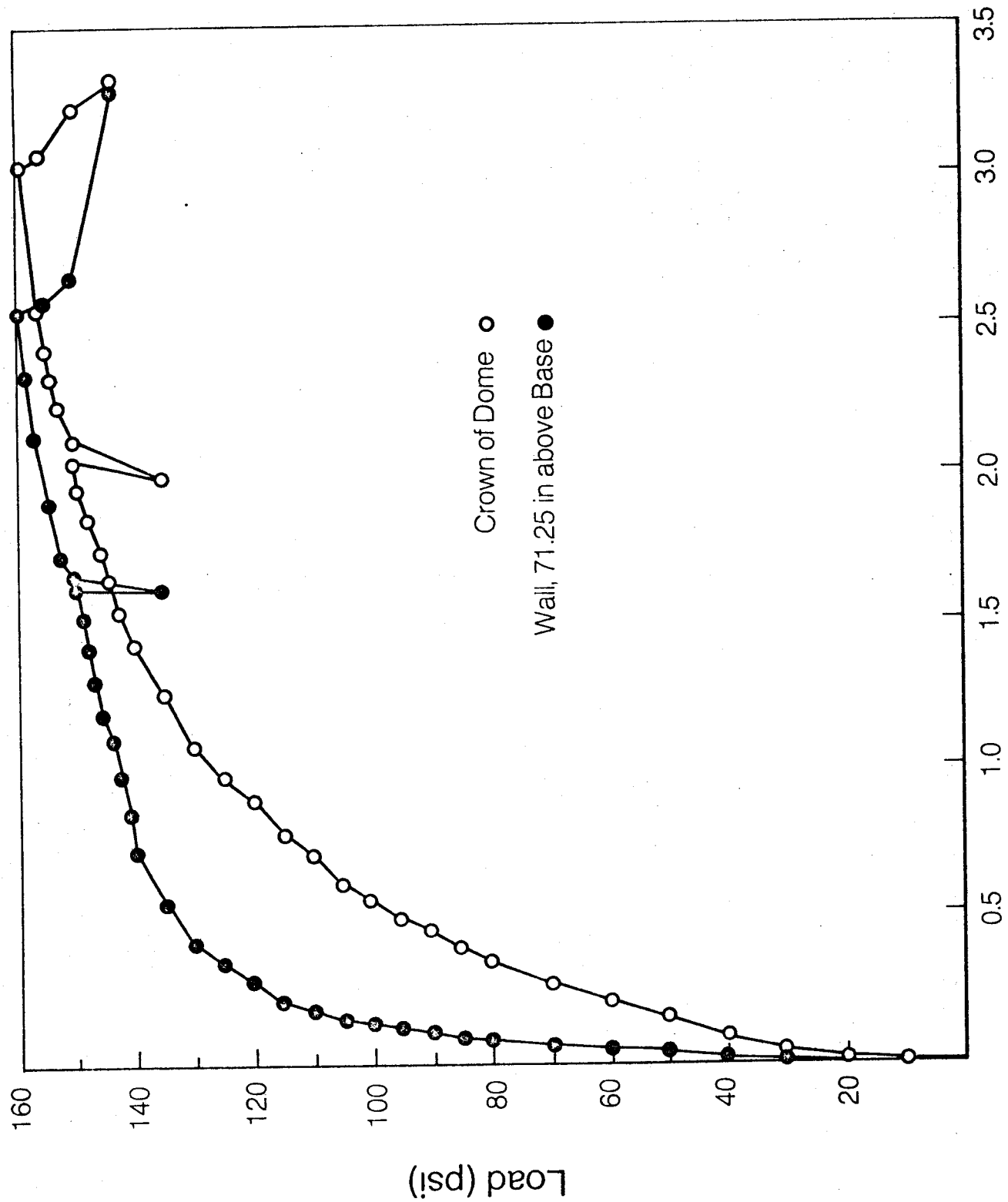

Figure 4.7 Pressure vs Deflection, Load Test G

Failure of the structure occurred at a pressure of 159.5 psi when the 7th horizontal tendon from the base and one vertical tendon fractured at midheight near the south-east buttress, permitting the liner to rupture. Immediately prior to failure the concrete cover over one of the horizontal tendon anchorages at this buttress was observed to pop outwards followed by rapid opening of the cracks in the immediate vicinity and spalling of the concrete. The failure region showing this spalling and the ruptured horizontal tendon is shown in Fig 4.8.

Although failure was due to fracture of tendons, the buttresses in which the horizontal tendons showed distress at loads well below the failure load. At 80 psi well defined horizontal cracks were visible across the face of the abutment and each anchorage point had a crack immediately above and below the anchor plates. These cracks continued to open and near 130 psi at several anchorages the concrete over the anchorage was spalled outwards and the anchor plates pulled into the sides of the buttresses. This effect can be seen in Fig 4.9 at a pressure of 135 psi. In general this condition became more serious with load. Typical of many of the anchorages are the two immediately above the failure zone above in Fig 4.8.

Prior to testing an analysis of the test structure was carried out using the technique described in Section 2 to predict deformations and strains. The agreement between predicted and measured values was generally good. Such a comparison for the deflections at midheight of the wall and crown of the dome are shown in Fig 4.10. Even better agreement was obtained between

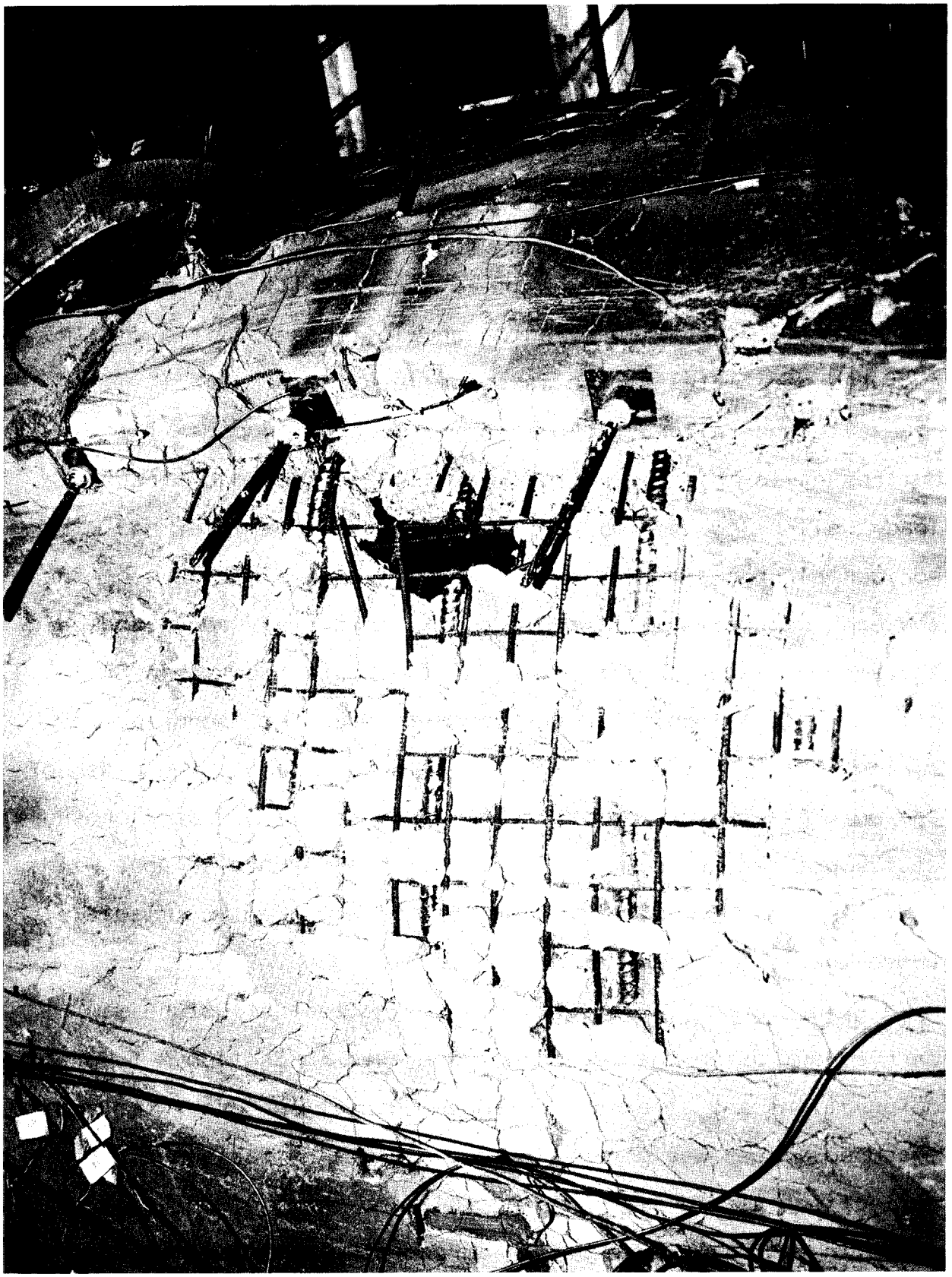

Figure 4.8 South Wall and South East Buttress after Failure

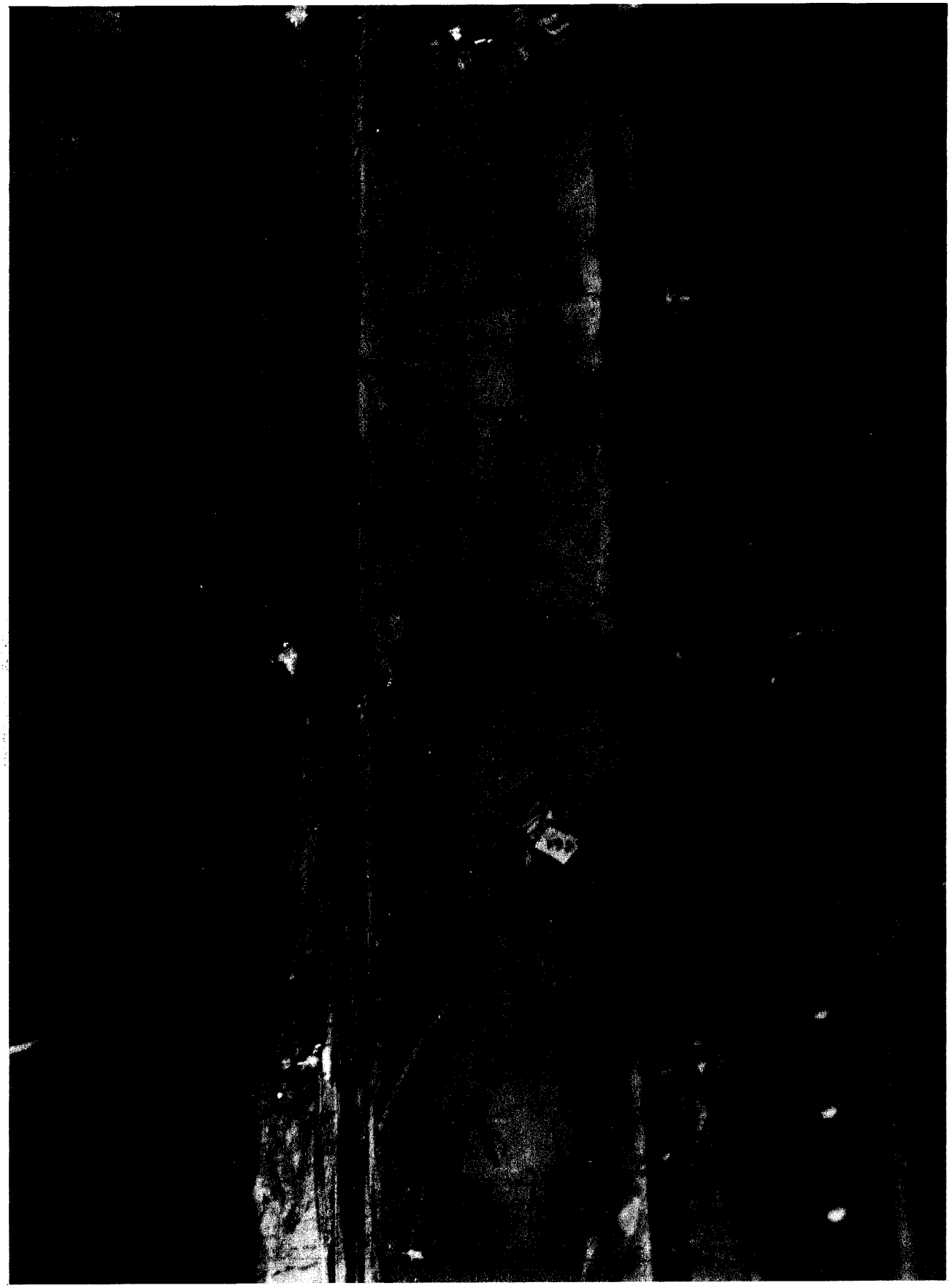

Figure 4.9 Cracking at Tendon Anchorages in Southwest Buttress at 135 psi

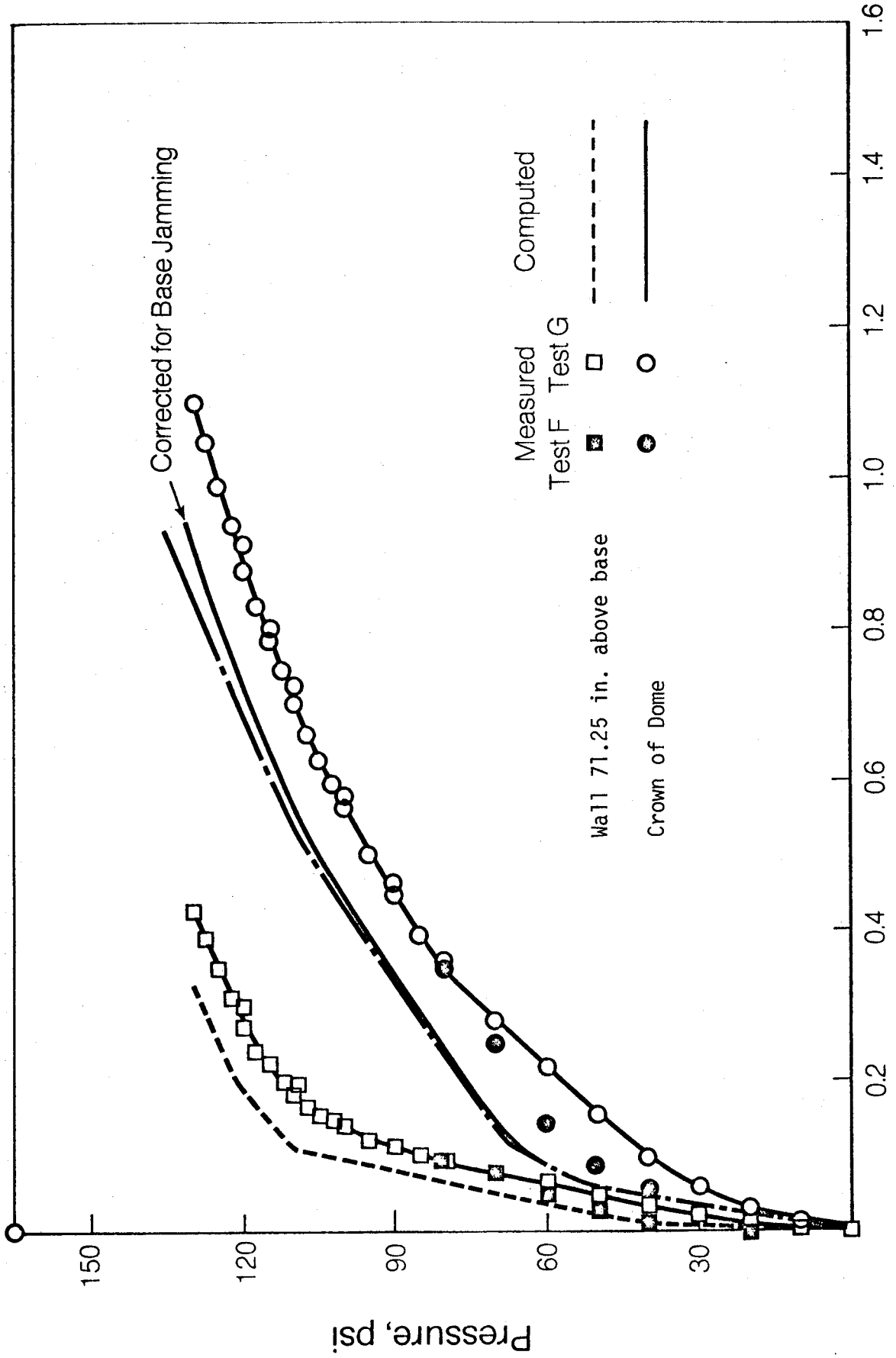

Figure 4.10 Measured and Computed Deflections for Wall and Dome, Line 1

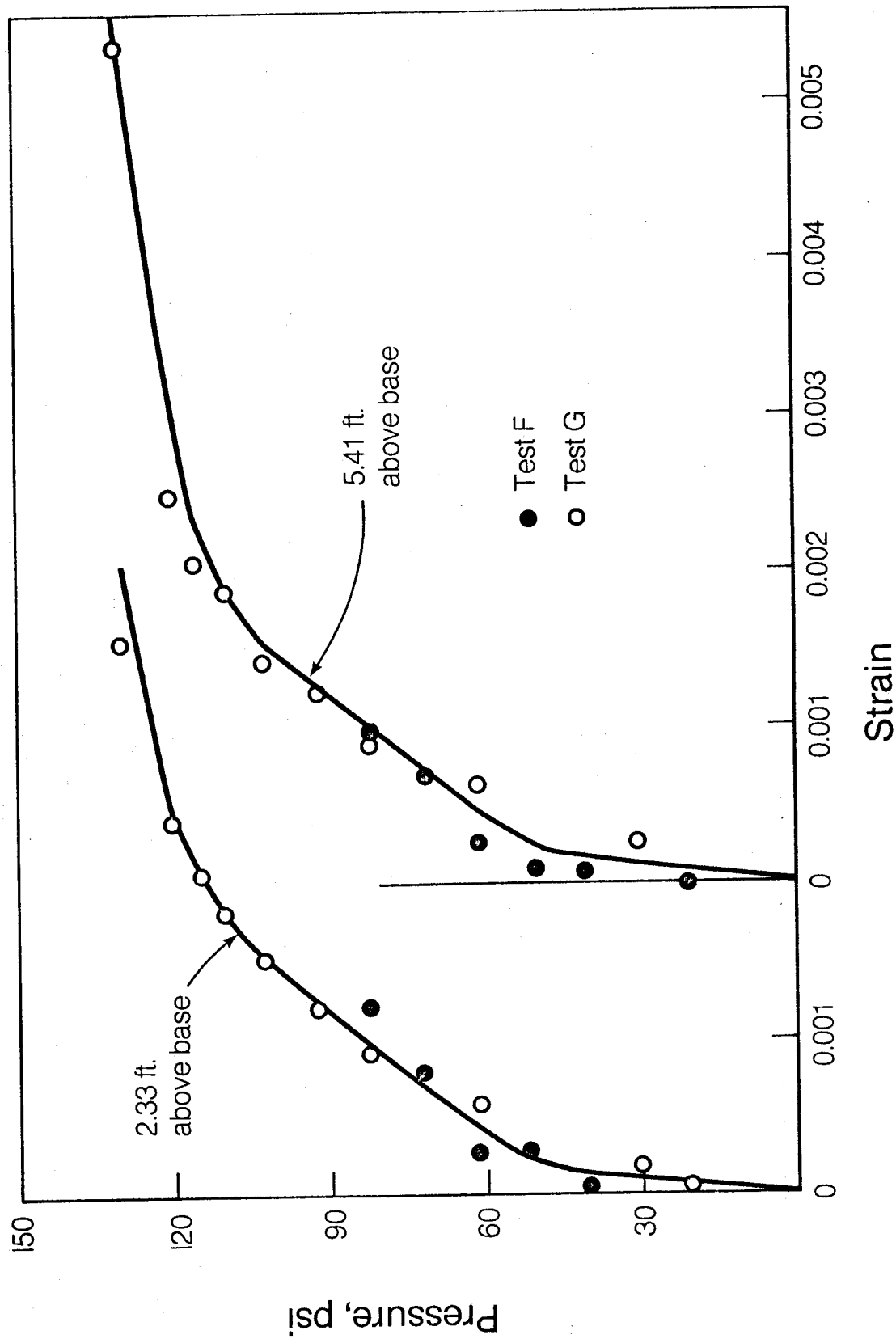

Figure 4.11 Measured and Computed Circumferential Strains at Surface of Wall

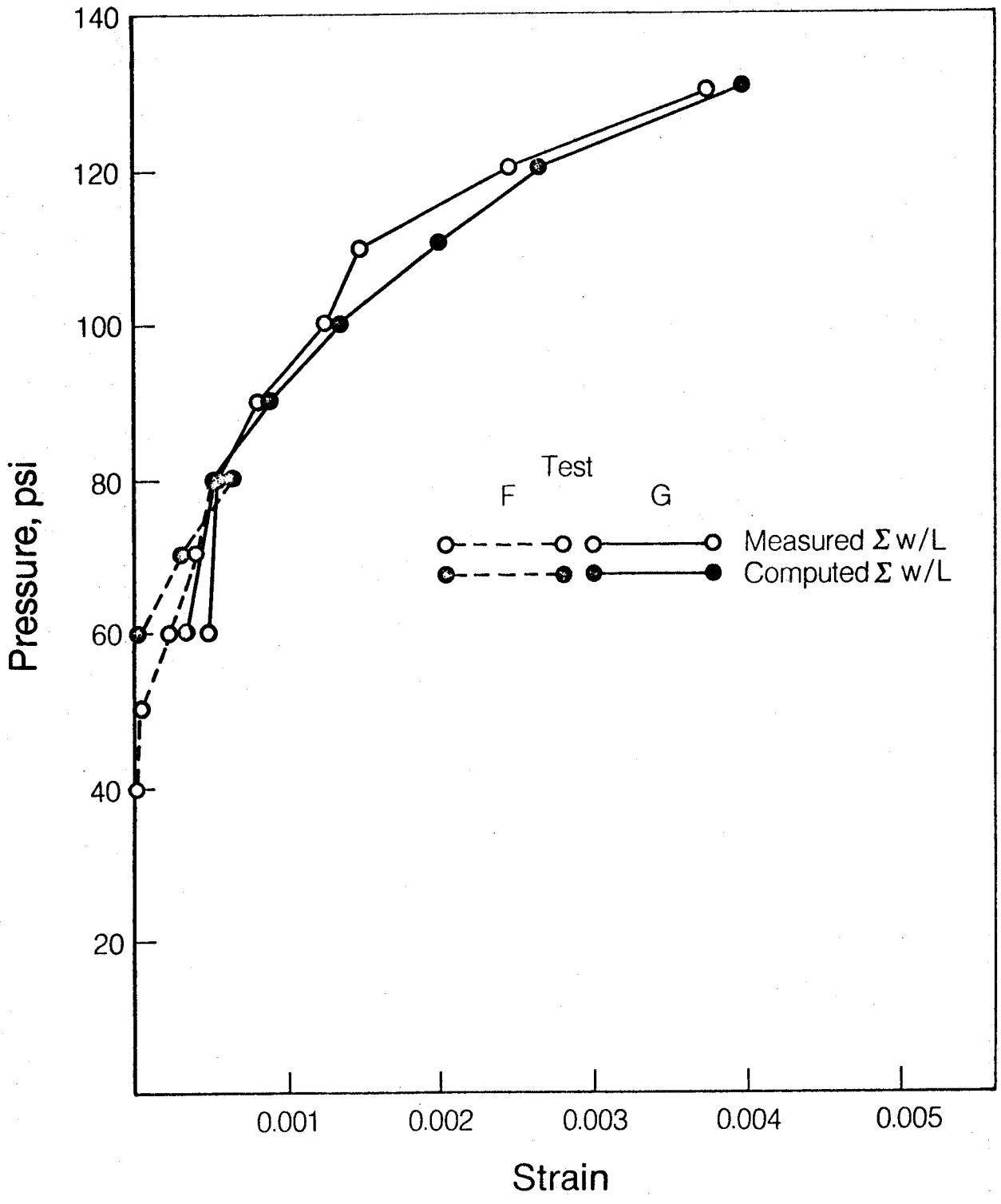

Figure 4.12 Measured and Computed Crack Strain, Vertical Cracks in Walls of Model Containment

measured and computed strains as shown in Fig 4.11.

Measured and computed values of $\Sigma w/L$ for the test structure computed by the technique described in Section 3.4 at different internal pressures are shown in Fig 4.12 to 4.14. The agreement between measured and computed values is sufficiently good that the procedures developed for predicting crack spacing and width have adequate accuracy for use in predicting overall response.

4.3 Behavior of Gentilly-2 Containment

From a study of the inelastic analysis of the Gentilly-2 containment and the observations of the test structure it is possible to predict with some degree of confidence the anticipated behavior of the Gentilly-2 containment if it were to be subjected to high overpressures.

The surface stresses at the proof test pressure, 20.7 psi, are given in Figs 4.15 and 4.16. In the meridional direction tension is indicated on the inside of the structure at the springing line of the dome and on the outside of the structure at the junction of the wall with the ring beam. However, both of these tensile stresses are below the cracking stress of 254 psi. Thus the analysis indicates that the structure satisfies the specific requirement that no cracking should occur under proof load. Although the lower dome was found to be cracked at this pressure, this does not affect leakage from the containment.

Pressure-displacement plots are given for points at the mid-height of the wall and the crown of the dome in Fig 4.17 and

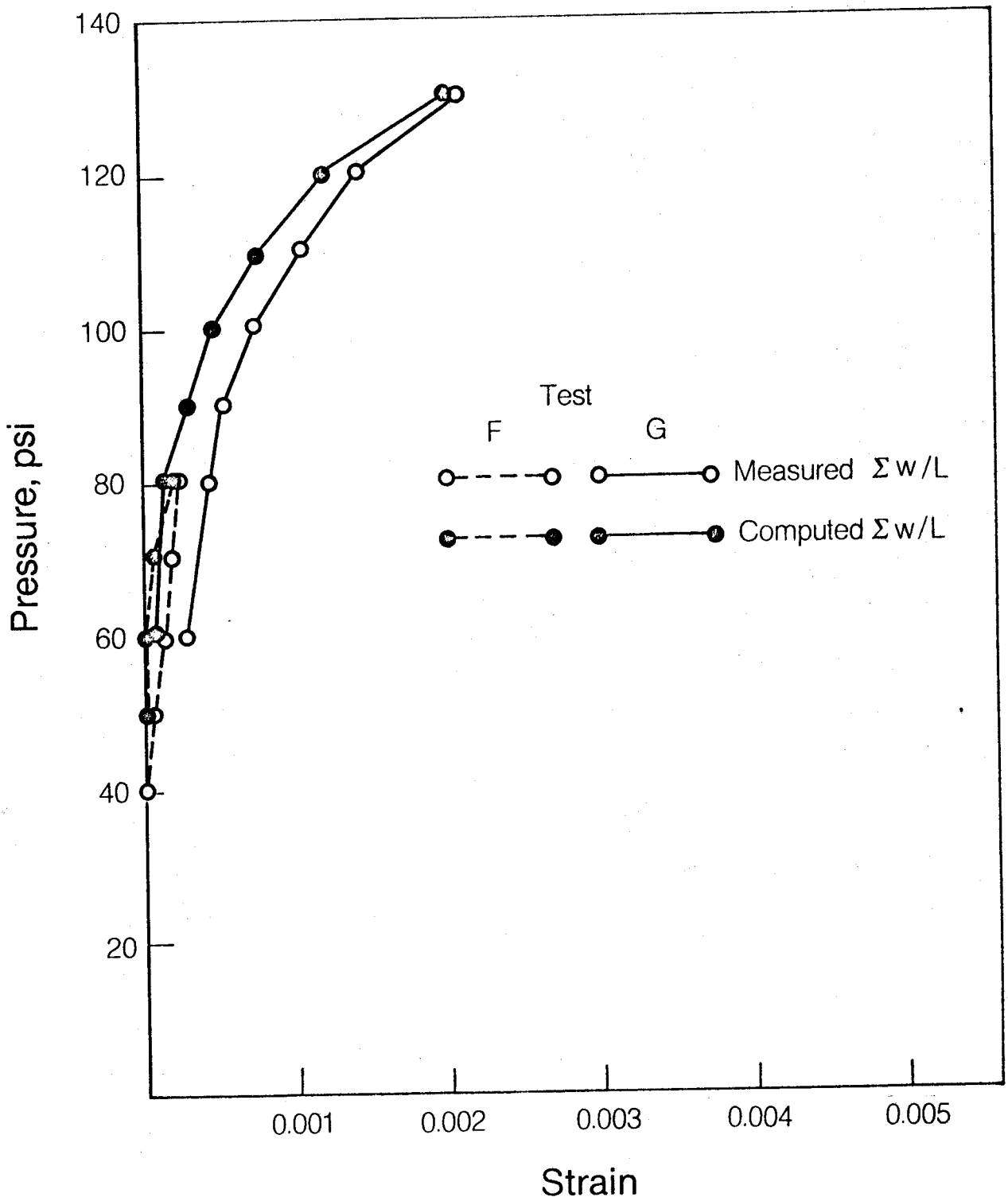

Figure 4.13 Measured and Computed Crack Strain Circumferential Cracks in Walls of Model Containment

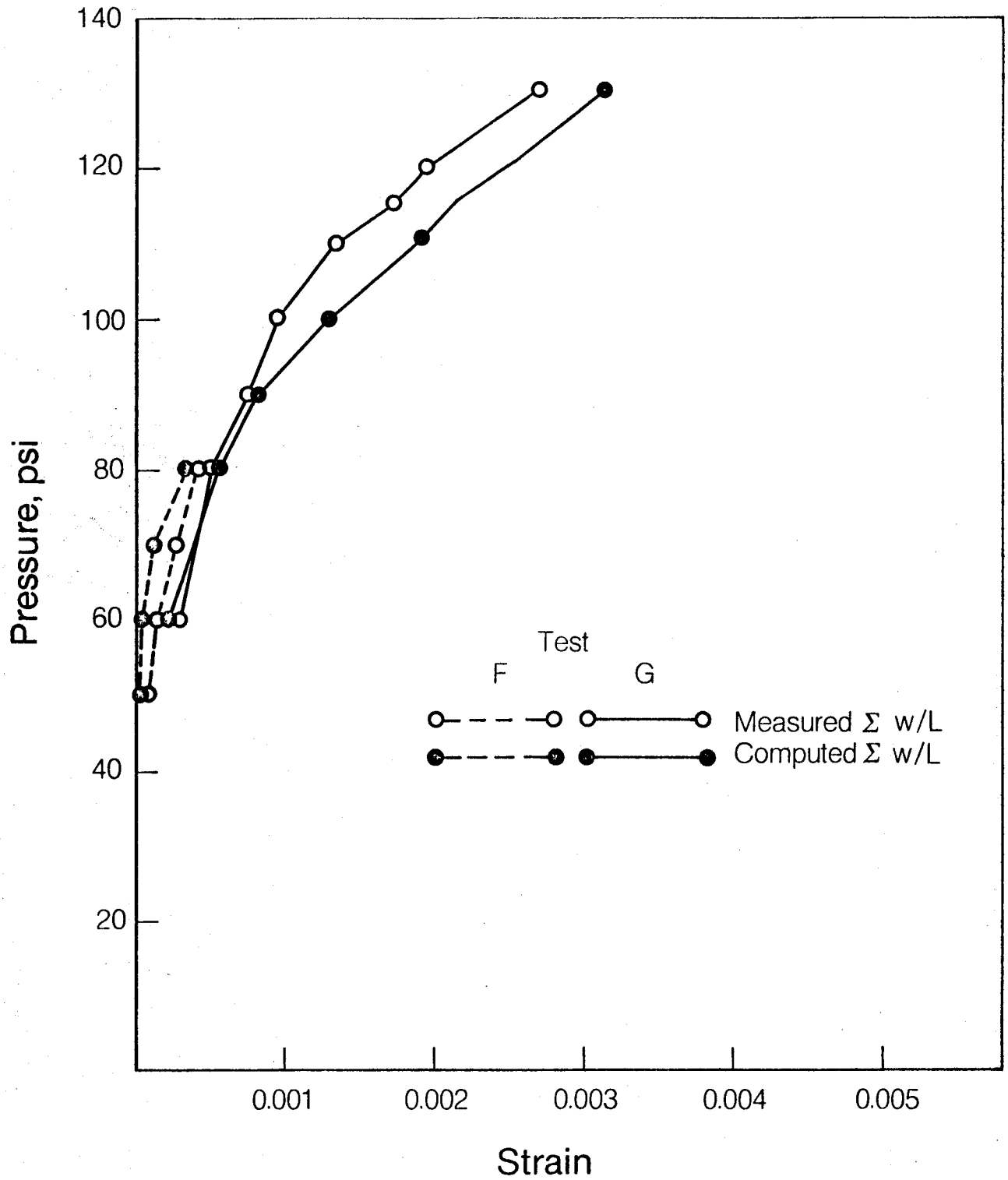

Figure 4.14 Measured and Computed Crack Strain, Meridional Cracks Crossing a Line Located 32 in. from Crown of Dome

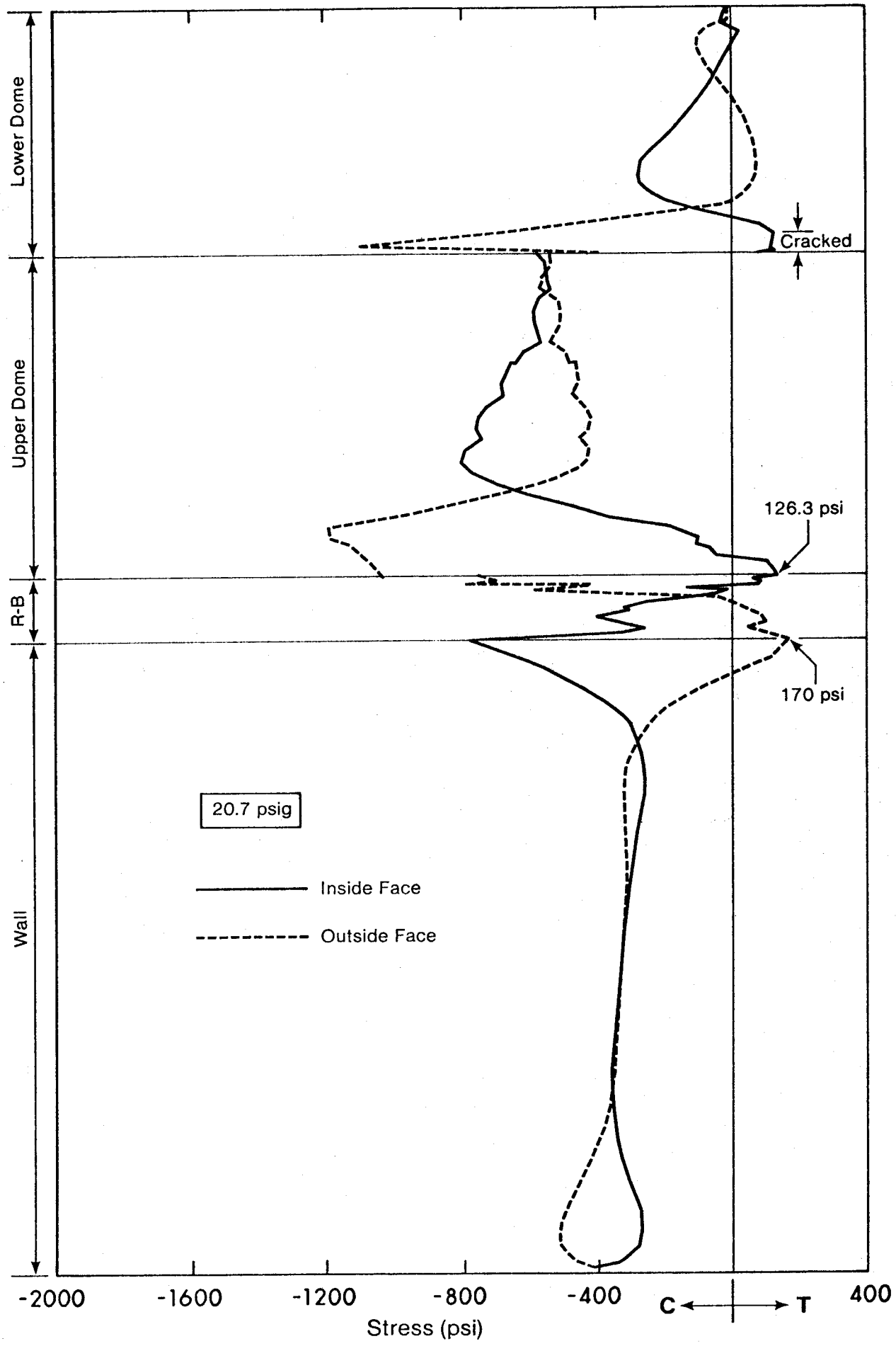

Figure 4.15 Meridional Surface Stresses in Gentilly-2 at Proof Pressure

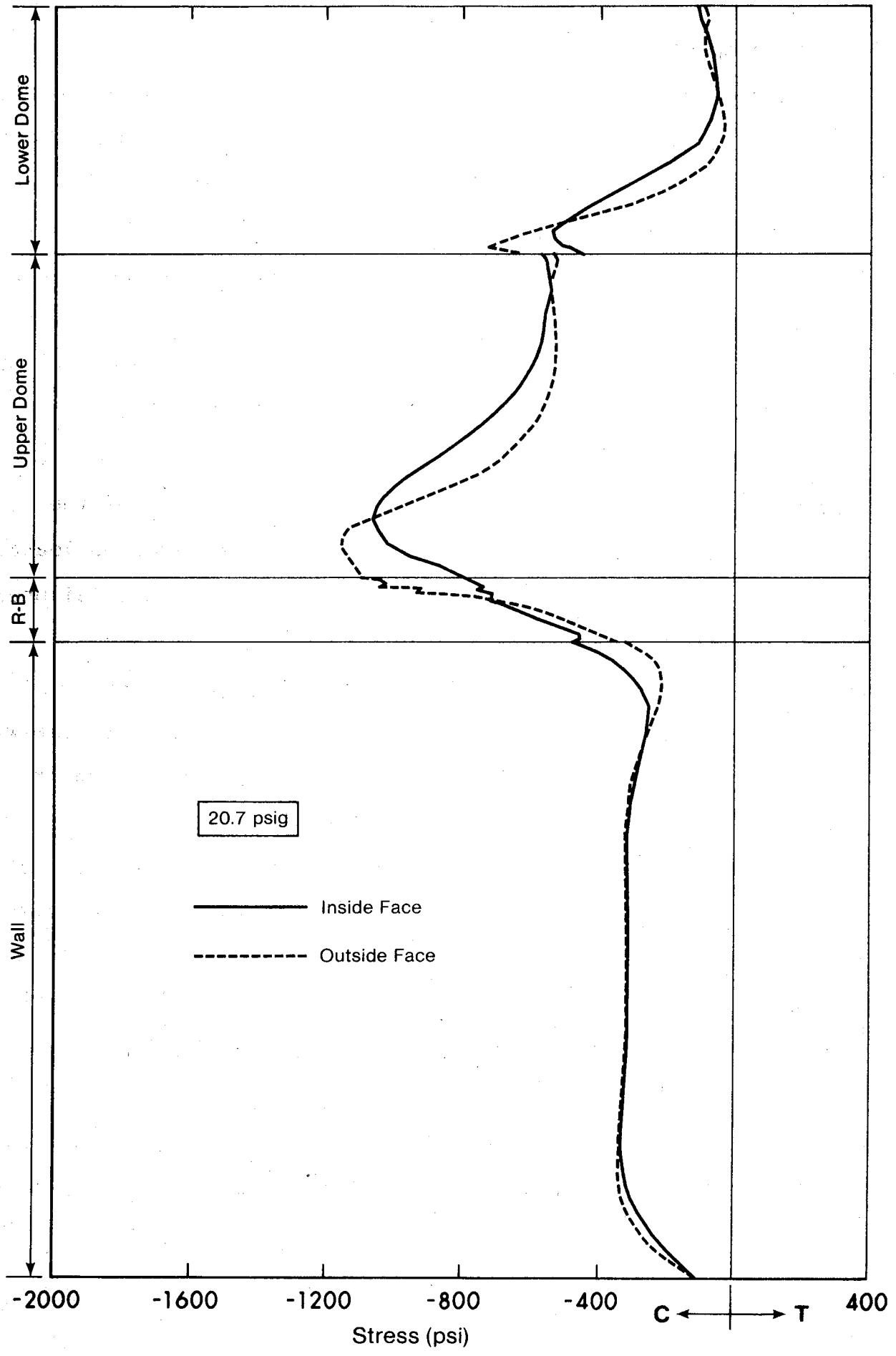

Figure 4.16 Circumferential Surface Stresses at Proof Pressure

4.18, respectively. The first cracking appears near the crown of the upper dome at approximately 48 psi in both the meridional and circumferential directions and quickly spreads over most of the dome surface. The first cracking in the wall are vertical cracks and appear at approximately 52 psi. No horizontal through-the-wall cracks are predicted prior to failure. The width of the vertical wall cracks increases quickly after yielding of the reinforcement at 66 psi. It is through these cracks that the majority of leakage would take place (see Section 5.2).

From the results of the analysis, the Gentilly-2 containment would fail at a pressure of 77.2 psi due to rupture of the horizontal tendons if the internal pressure considering leakage were to attain this value and there were no premature failures of the horizontal tendon anchorages.

The cracked moment of inertia of the buttress section is approximately 4 times that of a section of wall of the same width in the prototype and 9 times in the test structure. Outward movement of the buttresses in the test structure were approximately 60% of the movement of the wall between buttresses. Since the buttresses are less stiff relatively in the prototype it is expected that at high internal pressures there would be considerable outward bulging of the buttresses with the possibility of horizontal cracking across the buttress face in a manner similar to that observed in the test structure . When these are combined with the wedging action produced by the high compressive forces acting on the buttress edges from the tendon anchor plates, the possibility for anchorage failure exists.

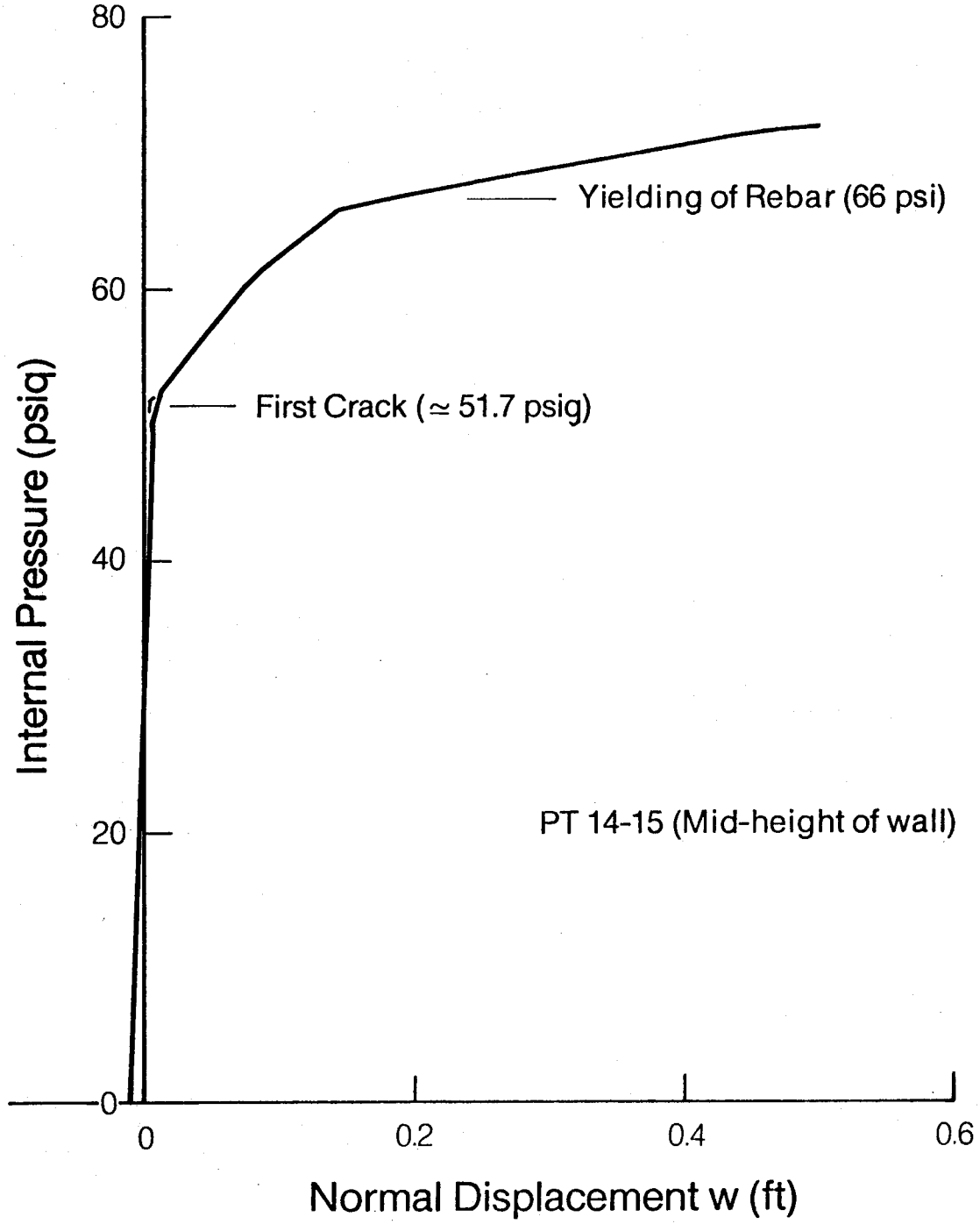

Figure 4.17 Pressure-Displacement at Mid-height of Wall of Gentilly-2

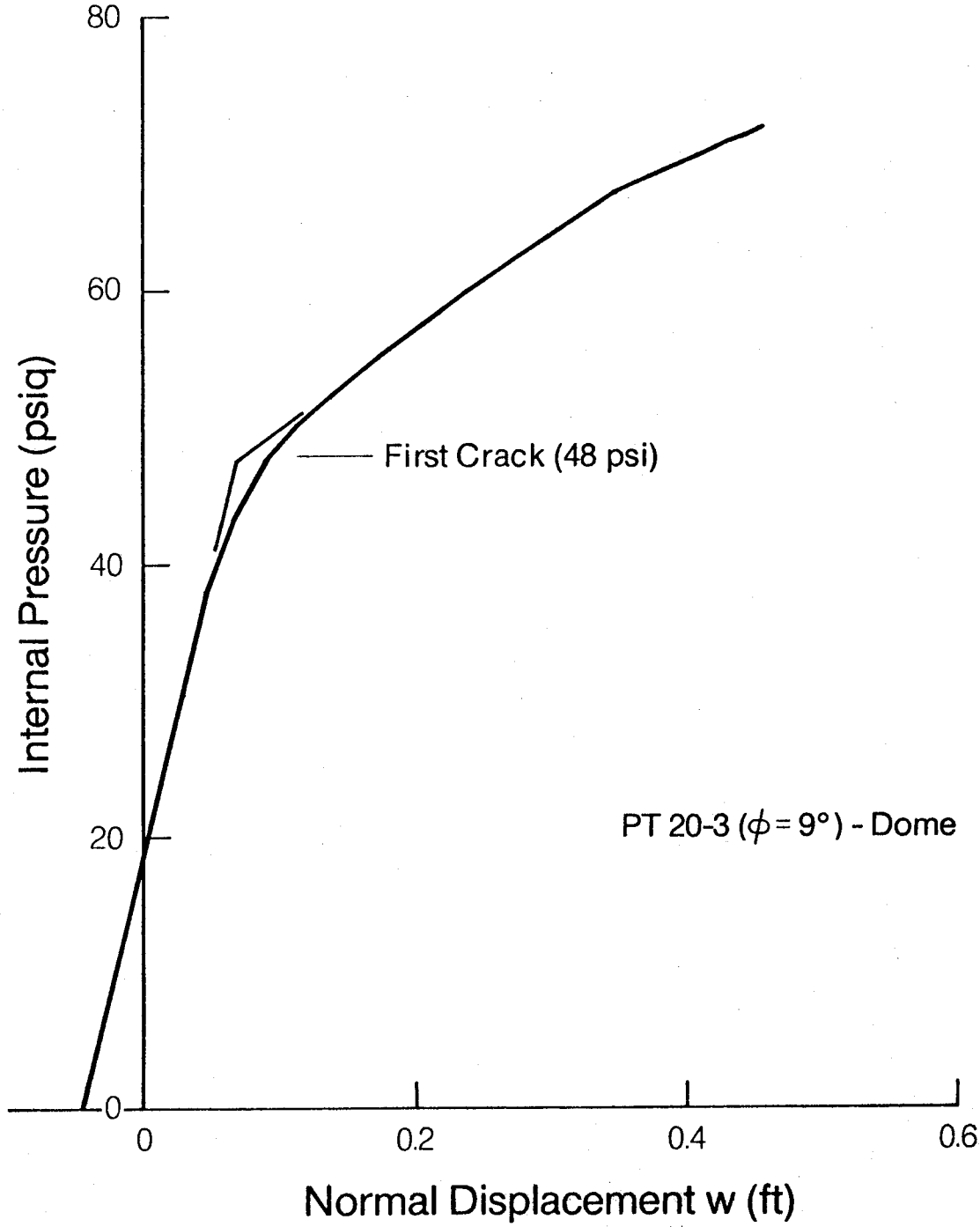

Figure 4.18 Pressure-Displacement at Crown of Dome of Gentilly-2

5. ESTIMATION OF LEAKAGE RATE

Once through-the-wall cracks form, there may be leakage of the pressurizing fluid through these cracks if the containment is not lined or if the liner ruptures. Procedures are presented in this section to predict the leakage of air through cracked concrete. In an actual containment the pressurizing fluid would be a mixture of air and steam. The methodology developed here for leakage of air should be applicable to other fluids if appropriate fluid constants are used.

5.1 Tests of Leakage Through Segments

To obtain a relationship between the degree of cracking and the corresponding leakage rate, two wall segments, Segments 10 and 14, were tested. These segments were identical in fabrication and loading to Segments 1 and 5, respectively, described in Section 3.1 except that provision was made to apply air under pressure to one face and to measure the volume of air passing through the segment.

In a containment structure the magnitude of the membrane stresses, and hence crack width, is a function of the internal pressure. In the leakage segment tests tensile membrane forces were applied to the reinforcement protruding from the edges and the air pressure was obtained by the use of pressure chambers constructed over the segment faces. In this situation the tensile forces may be varied independently of the applied pressures. The tensile forces applied to the segment were increased in increments to 95% of the ultimate strength of the tendons

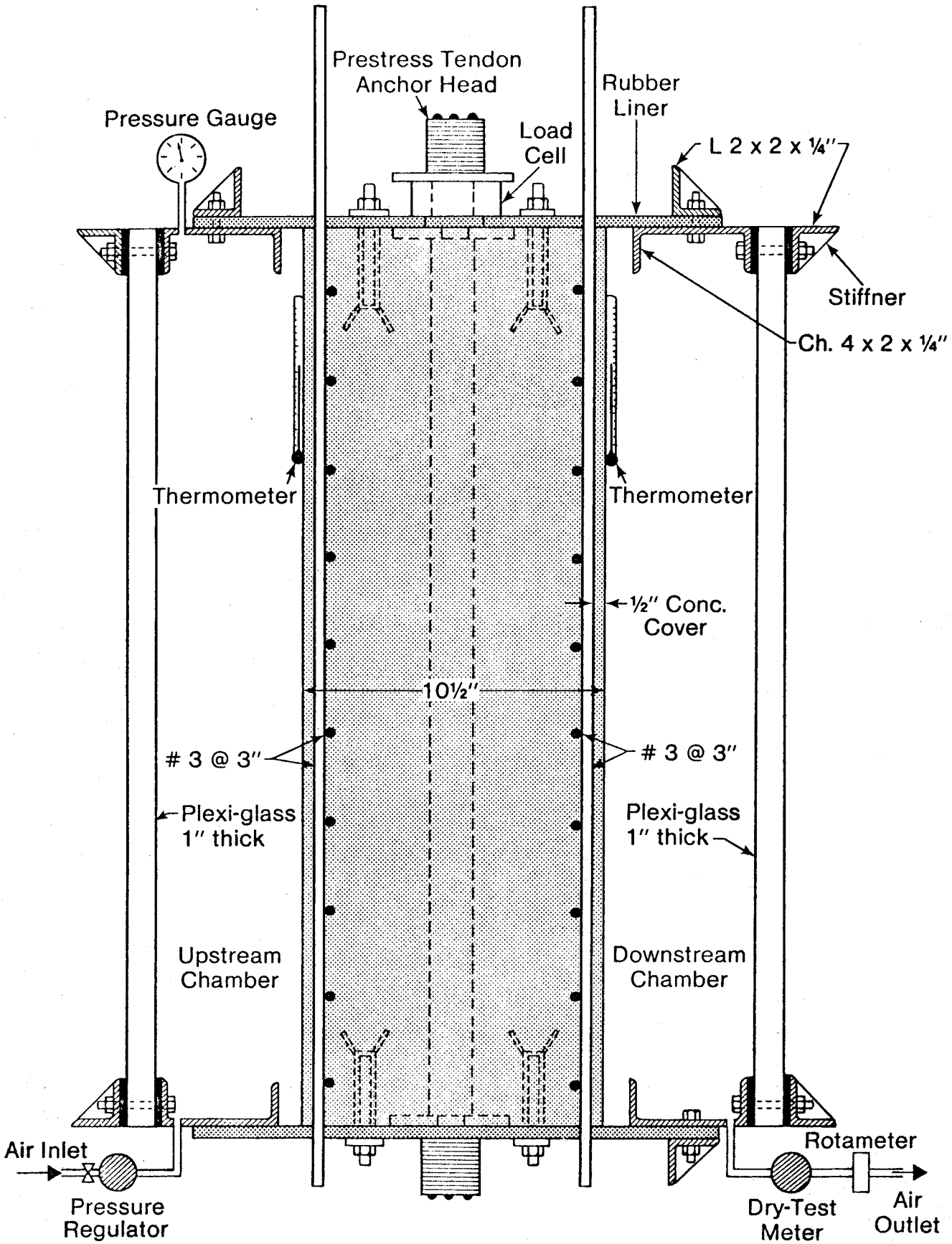

Figure 5.1 Details of Air Chambers and Rubber Liners, Segment 10

ensuring that significant through-the-wall cracking ocurred. The maximum air pressure that could be maintained was dependent on the amount of air that could be supplied to the upstream chamber and the rate of leakage. Thus for a given tensile force, and hence crack width, it was possible to measure the leakage rate at different pressure levels, thereby providing a means of verifying the theoretical prediction of leakage rate.

The testing procedures and instrumentation for Segments 10 and 14 were similar to the corresponding Segments 1 and 5, except that due to the presence of the pressure chambers the widths of cracks could not be measured. However it was observed that the crack patterns and average steel strains measured from embedded electric resistance strain gages in the leakage segments agreed closely with those in the corresponding segments in which crack widths were measured. Hence it was assumed in assessing leakage rates that the crack widths measured in Segments 1 and 5 also applied to Segments 10 and 14, respectively.

Details of the construction of the pressure chambers are given in Ref 6. Leakage of air through the edges of the segments was prevented by a rubber frame that was placed over the edges and to which the pressure chambers were bolted. Air passing through the specimen from the upstream face to the downstream face was collected on the downstream face and measured with a flow meter when exhausted to atmosphere. In Segment 10 there was considerable difficulty in developing any significant pressure on the upstream face because of the degree of leakage from the edges of the segment. This was caused in part from the many holes

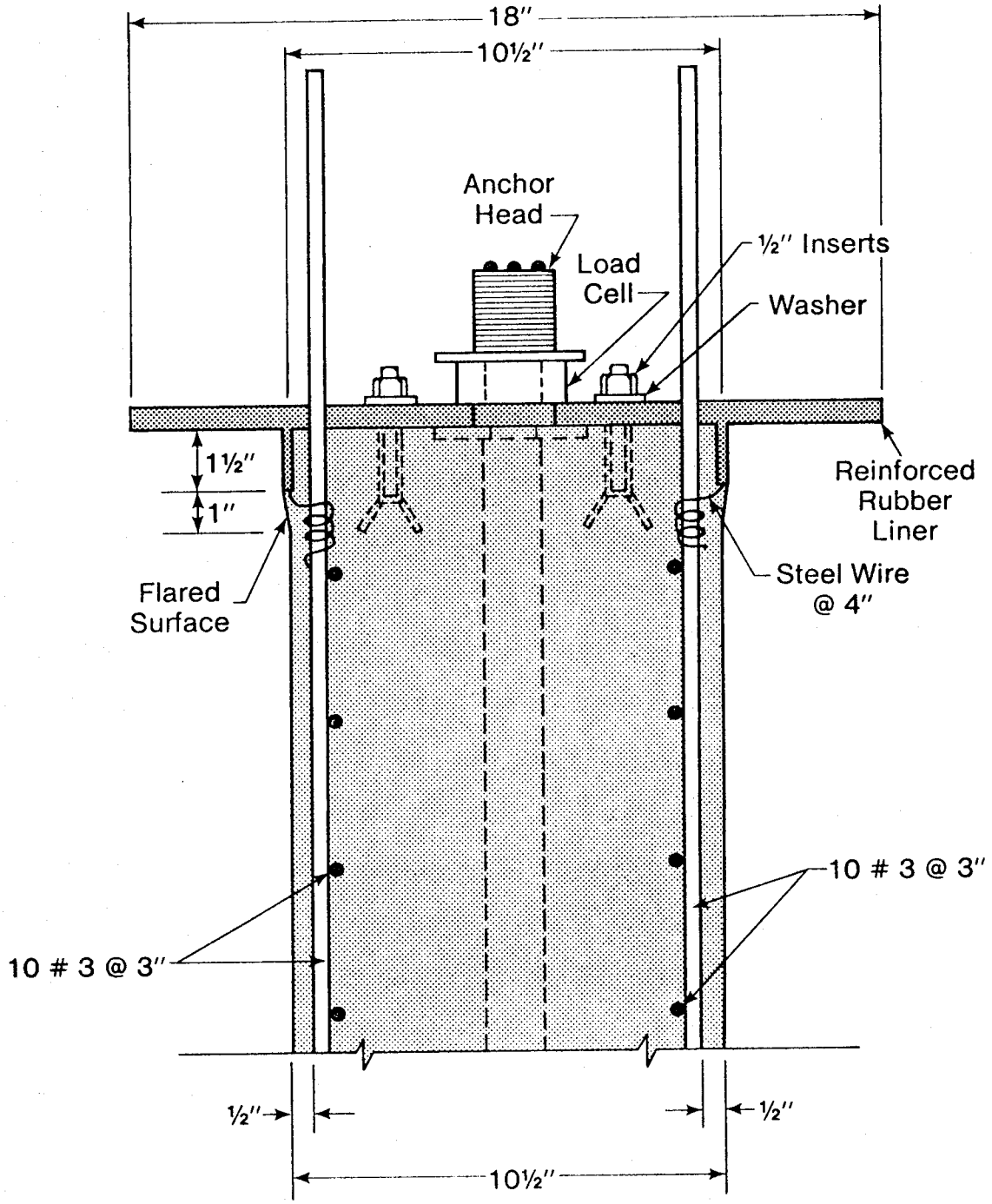

Figure 5.2 Details of Rubber Liner, Segment 14

punched in the rubber seal to accommodate the steel reinforcement and prestressing tendons protruding from the edges of the specimens, and partly by air passing between the rubber seal and the edges of the segment. Based on the experience gained in testing Segment 10, the rubber frame and pressure chamber connections were modified for Segment 12. In this latter test there was no significant leakage from or around the edges of the segment and the maximum pressure that could be applied was limited only by the rate at which air could be supplied to the upstream chamber. A cross-section through Segment 10 showing the air chambers is given in Fig 5.1 and the modification to the rubber seal is shown in Fig 5.2.

5.2 Computation of Leakage Rate

If the flow through a concrete crack is idealized as the flow through the gap between two parallel plates and the friction coefficient factor is constant along the length of the flow path, then from theoretical considerations, (6), the total flow of air through a cracked segment with j cracks is given by the expression:

$$Q = p \frac{4}{k\mu} \sum_{i=1}^{j} \frac{B_i W_i^3}{L_i} \qquad (5.1)$$

where:

Q = rate of flow through a group of cracks, ft /sec

p = pressure gradient

$$= \frac{P_1^2 - P_2^2}{P_1}$$

P_1 = absolute air pressure at upstream face lb/ft^2

P_2 = absolute air pressure at downstream face lb/ft^2

μ = viscosity of air, lb.sec/ft

B_i = length of crack i parallel to surface, ft.

L_i = length of crack i perpendicular to surface, ft

W_i = width of crack i, ft

K = dimensionless constant

The dimensionless constant, K, is dependent on the wall friction and must be determined from tests.

To use Eqn. 5.1 it is necessary to know the extent and width of every through-the-wall crack, a condition not practical when attempting to predict leakage through containment walls. To extend the theoretical formulation to concrete sections in order to permit evaluation of K from the segment tests involved the following reasoning.

The length of all cracks, L, is taken as the wall thickness and hence for any wall section will be constant. This permits L to be taken outside the summation sign. Similarly B may also be considered as known and constant for a given loading. Thus Eqn. 5.1 can be rewritten as:

$$Q = p \frac{4}{k\mu} \frac{B}{L} \sum_{i=1}^{j} w_i^3 \qquad (5.2)$$

$$= \frac{p}{C} \sum_{i=1}^{j} w_i^3$$

where $$C = \frac{k\mu L}{4B} \qquad (5.3)$$

To eliminate the need to consider widths of individual cracks the concept of an equivalent or representative crack width, w, is introduced. This is the mean crack width evaluated in Section 3.3. If B is taken as the extent of all equivalent cracks then:

$$w^n = \sum_{i=1}^{j} w_i^3 \qquad (5.4)$$

where the exponent n must be evaluated from tests. In keeping with the concept of an equivalent crack, regardless of the value, w^n will be a constant at a given load level. Equation 5.2 can now be written as:

$$Q = \frac{p}{C} w^n \qquad (5.5)$$

or

$$P = \frac{C}{w^n} Q = DQ \qquad (5.6)$$

The above reasoning would be verified if a plot of p vs Q should result in a straight line for all levels of applied load. The slope of this line at any load level and hence crack width, w, would relate the flow rate, Q to the pressure gradient, p. Such plots are given in Fig 5.3 for Segment 14. Due to problems in sealing the perimeter of Segment 10 the results of that test were not used. It is seen from Fig 5.3 that there is a reasonably linear relationship between p and Q from the test data.

At any given load and hence crack width, the constant of proportionality, D, can be expressed as:

$$\ln D = \ln C - n \ln w \qquad (5.7)$$

A plot of this equation on log-log paper should result in a

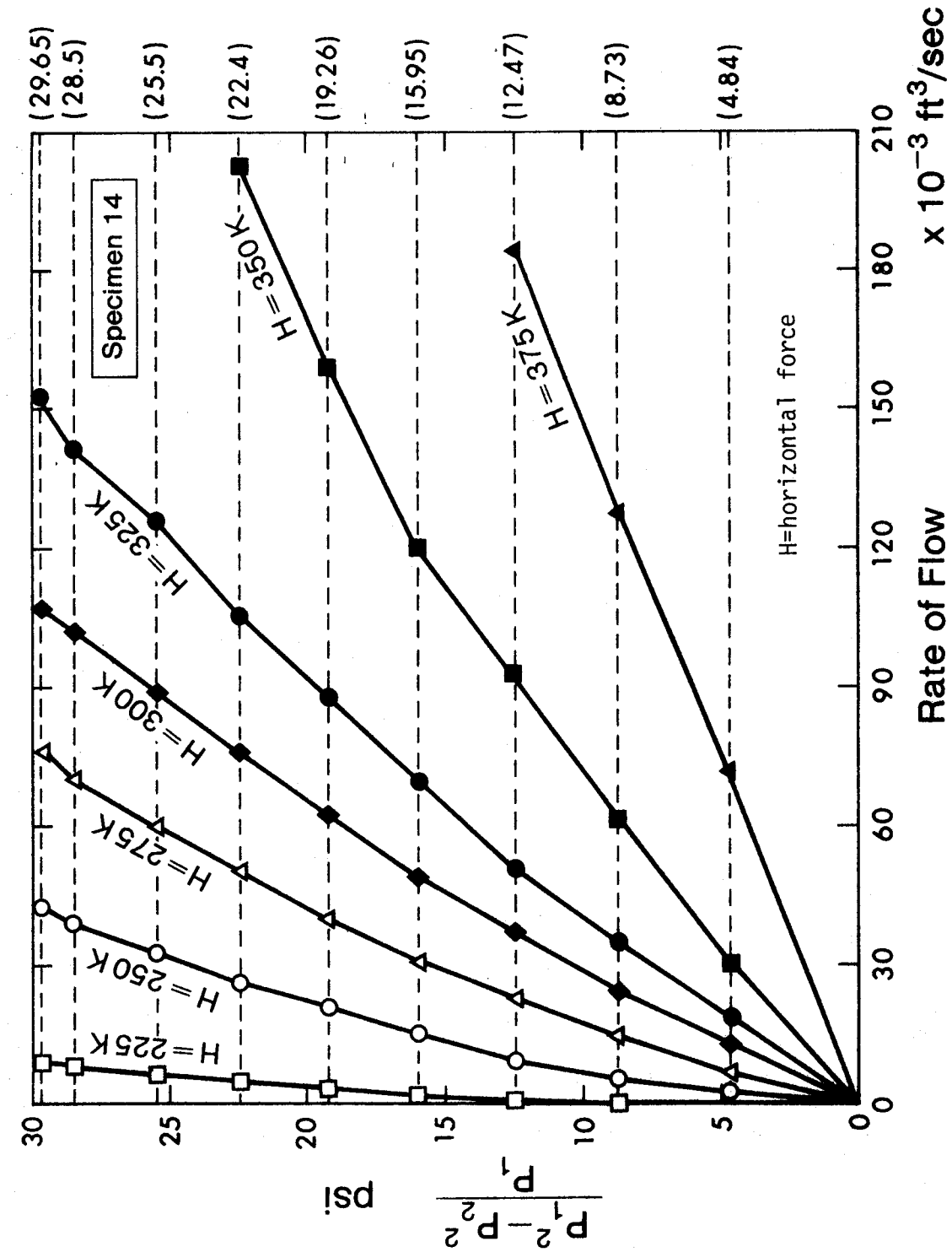

Figure 5.3 Flow Rate - Pressure Gradient Relationship for Segment 14

straight line, the slope of which is the exponent n. Such a plot for Segment 14 is given in Fig 5.4 and the value of n is seen to be 3. The linear plot verifies the concept of replacing a statistical population of crack widths with an equivalent crack width equal to the mean and the slope of the plot indicates the power of the equivalent crack width is the same as for individual cracks. The constant, C, can be evaluated from Eqn. 5.6 for any load level. Values of C for Segment 14 ranged from 1.638×10^{-6} to 2.233×10^{-6} lbf.sec/ft^2 with an average of 1.86×10^{-6} lbf.sec/ft^2 .

For Segment 14 the total length of cracking, B, was taken as the average of crack lengths measured on the two surfaces after failure (11.9 ft). The length of crack, L, was taken as the segment thickness, (0.875 ft). At 70 F, using the viscosity of air as $0.,38 \times 10^{-6}$ lb sec/ft^2, the value of K from Eqn. 5.3 is 267.

K is a dimensionless constant which is a measure of the wall roughness and may be considered to apply to all concrete cracks. Hence, for a given structure, if the extent of cracking, ie, B and L, is known the constant C for that load level can be computed from Eq. 5.3.

5.3 Predicted Leakage from Gentilly-2 Type Containments

The procedures developed can be used to estimate the rate of leakage of the Gentilly-2 containment. The reader is cautioned that the values presented are based on limited experimental data using air as the pressurizing fluid.

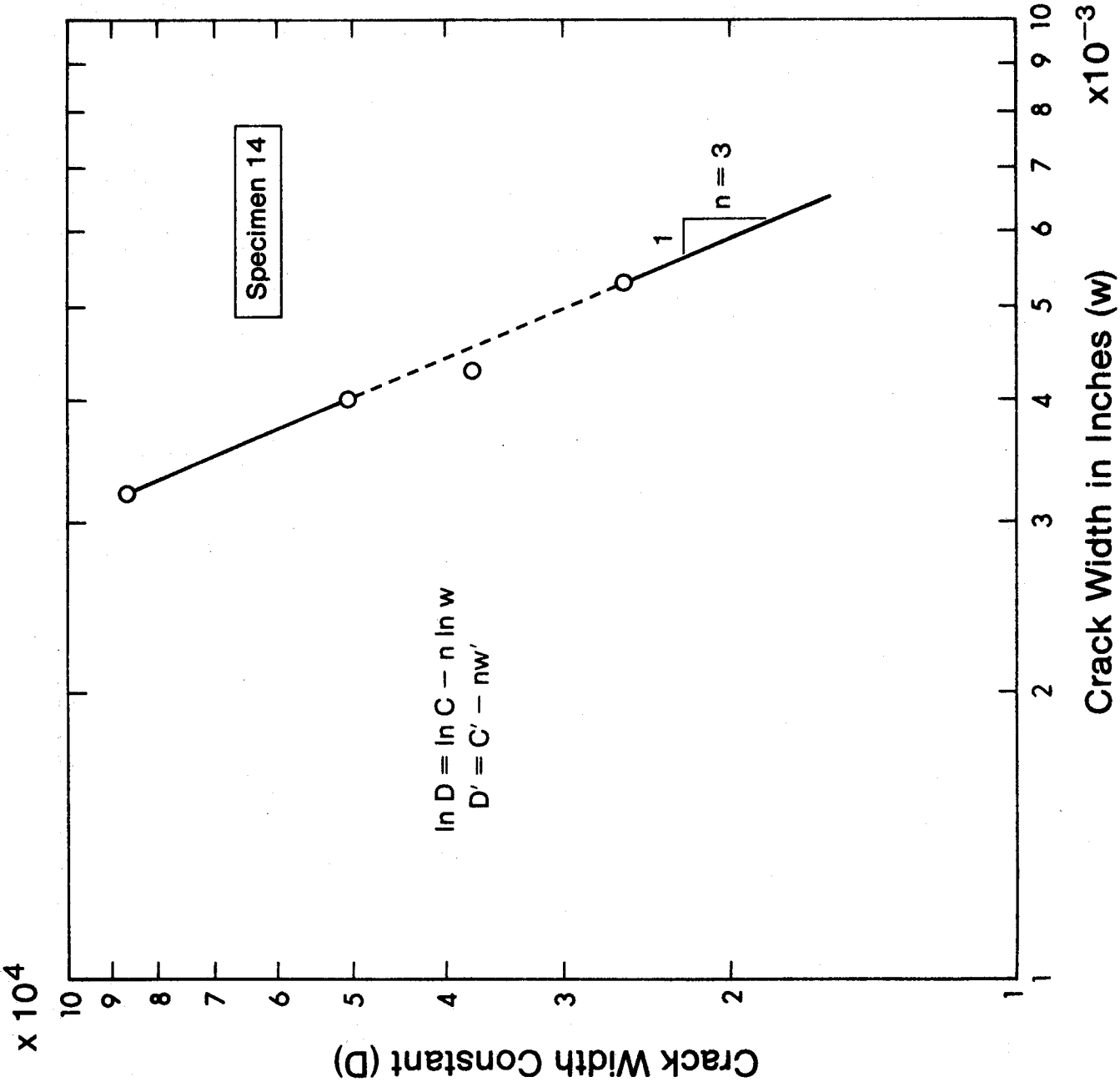

Figure 5.4 Relationship between D and Crack Width, Segment 14

reinforcement and prestress. Thus the surface is divided into representative areas and an equivalent crack width is computed for each area using the procedures outlined in Section 3.3. The number and hence extent, B, of the cracking in each area is determined from the spacing of the cracks and the dimensions of the structure. The crack length, L, is taken as the thickness of the section. This permits evaluating the constant, C, for any representative area. With the value of C and the equivalent crack width w, the leakage from each representative area may be computed for any pressure gradient using Eqn. 5.5. The rates for each area may be added to obtain the total leakage rate for the structure. The above procedure is discussed in detail in Reference 10.

Leakage rates for the Gentilly-2 containment were computed at internal pressures of 50, 60, 64, 67, 70 and 72.125 psig and the results presented in Fig 5.5. It is seen that for internal pressures below 50 psig, more than twice the design accident pressure, there is no appreciable leakage from the containment. As the reinforcement begins to yield, the cracks open and the rate of leakage increases exponentially. At a pressure of 72 psi, approximately 93% of the ultimate strength of the structure, the computations indicate a leakage approximately equal to the volume of the structure each second.

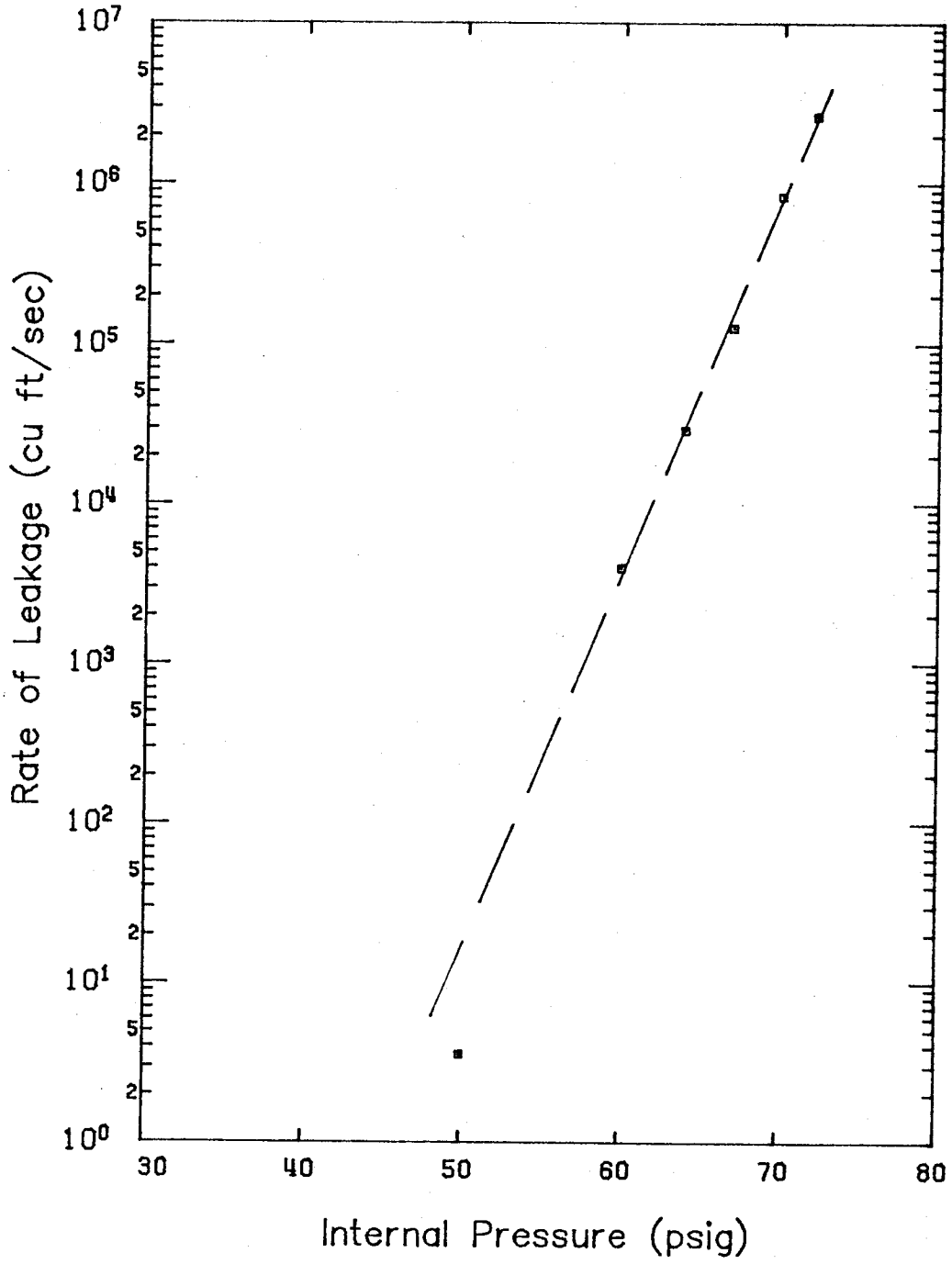

Figure 5.5 Estimated Leakage Rate for Gentilly-2 Containment

6. SUMMARY

This report presents the most significant findings of a study to assess the response of circular prestressed concrete secondary containment structures for nuclear reactors when subjected to high internal overpressures. A computer analysis is described for computing the strains and deflections at various points in the structure. Experimentally derived relationships between the strains and crack spacing, crack width and leakage are given. These procedures were applied to the Gentilly-2 secondary containment building. It was found that for this building, cracks would first penetrate through the wall at 48 psi internal pressure, or 2.3 times the proof test pressure. After extensive inelastic deformation, failure would occur at 77 psi. This assumes that the pressurizing medium could be supplied rapidly enough to maintain these pressures. Leakage calculations indicate that leakage through cracks would be negligible at pressures below 50 psi, increasing exponentially as the pressure increased above that value. At 93 percent of the predicted failure load the calculations indicate a leakage rate approximately equal to the volume of the structure each second.

REFERENCES

(a) University of Alberta Structural Engineering Reports on this project.

1. Epstein, M. and Murray, D.W., "An Elastic Stress Analysis of a Gentilly Type Containment Structure: Volume 1", Structural Engineering Report No. 55, Department of Civil Engineering, University of Alberta, Edmonton, Canada, April 1976.
2. Rohardt, A.M., Murray, D.W., and Simmonds, S.H., "A Classical Flexibility Analysis for Gentilly Type Containment Structures", Structural Engineering Report No. 63, Department of Civil Engineering, University of Alberta, Edmonton, Canada, June 1978.
3. Murray D.W., "Some Elementary Mechanics of Explosive and Brittle Failure Modes in Prestressed Containments", Structural Engineering Report No. 66, Department of Civil Engineering, University of Alberta, Edmonton, Canada, June 1978.
4. Murray, D.W., Chitnuyanondh, L., Wong, C., and Rijub-Agha, K.Y., "Inelastic Analysis of Prestressed Concrete Secondary Containments", Structural Engineering Report No. 67, Department of Civil Engineering, University of Alberta, Edmonton, Canada, July 1978.
5. Chitnuyanondh, L., Rizkalla, S., Murray, D.W. and MacGregor, J.G., "An Effective Unianial Tensile Stress-Strain Relationship for Prestressed Concrete", Structural Engineering Report No. 74, Department of Civil Engineering, University of Alberta, Edmonton, Canada, February 1979.

6. Rizkalla, S.H., Simmonds, S.H. and MacGregor, J.G., "Leakage Tests of Wall Segments of Reactor Containments", Structural Engineering Report No. 80, Department of Civil Engineering, University of Alberta, Edmonton, Canada, October 1979.
7. Simmonds, S.H., Rizkalla, S.H., and MacGregor, J.G., "Tests of Wall Segments from Reactor Containments", Structural Engineering Report No. 81, Department of Civil Engineering, University of Alberta, Edmonton, Canada, November 1979.
8. MacGregor, J.G., Rizkalla, S.H., and Simmonds, S.H., "Cracking of Reinforced and Prestressed Concrete Wall Segments", Structural Engineering Report No. 82, Department of Civil Engineering, University of Alberta, Edmonton, Canada, March 1980.
9. MacGregor, J.G., Simmonds, S.H., and Rizkalla, S.H., "Test of a Prestressed Concrete Secondary Containment Structure", Structural Engineering Report No. 85, Department of Civil Engineering, University of Alberta, Edmonton, Canada, March 1980.
10. Murray, D.W., Wong, C., Simmonds, S.H., and MacGregor J.G., "An Inelastic Analysis of the Gentilly-2 Secondary Containment Structure", Structural Engineering Report No. 86, Department of Civil Engineering, University of Alberta, Edmonton, Canada, April 1980.

(b) Published Papers Arising From This Project

11. Epstein, M., Rkjub-Agha, K., and Murray, D.W., "A Two-Parameter Constitutive Law For Axisymmetric Shell

Analysis", Symposium on Applications of Computer Methods in Engineering, University of Southern California, Los Angeles, California, August 23-26, 1977.

12. Epstein , M. and Murray, D.W., "A Biaxial Law for Concrete Incorporated in the BOSOR5 Code", Computers and Structures, Vol. 9, No. 1, July 1978, pp. 57-63.
13. Murray, D.W., "A Review of Explosive Characteristics of Prestressed Secondary Containments Near the Ultimate Load", Nuclear Engineering and Design, Vol. 52, Amsterdam, 1979.
14. Chitnuyanondh, L, Rizkalla, S.H., Murray, D.W., and MacGregor, J.G., "Effective Tensile Stiffening in Prestressed Concrete Wall Segments", Paper J3/4, SMIRT5, Berlin, 1979.
15. Murray, D.W., Chitnuyanondh, L., and Wong, C., "Modelling and Predicting Behavior of Prestressed Concrete Secondary Containment Structures Using BOSOR5", Paper J3/5, SMIRT5, Berlin, 1979.
16. Murray, D.W., Simmonds, S.H., MacGregor, J.G., "Some Aspects of Structural Response of Concrete Containment Buildings To Accident Conditions", Meeting, Canadian Nuclear Association, Toronto, May, 1979.
17. Rizkalla, S., Simmonds, S.H., and MacGregor, J.G., "A Test of a Model of a Thin-Walled Prestressed Concrete Secondary Containment Structure", Paper J4/2, SMIRT5, Berling, August 1979.
18. Simmonds, S.H., Murray, D.W., MacGregor, J.G., and Rizkalla, S.H., "Behavior of Prestressed Concrete Containment Structures Due to Overpressure", Proceedings of the Canadian

Structural Concrete Conference, Banff, May 1979.

(c) Papers and Reports Based on Data Gathered in This Project

19. Koziak, B.D.P., and Murray, D.W., "Analysis of Prestressed Concrete Wall Segments", Structural Engineering Report No. 78, Department of Civil Engineering, University of Alberta, Edmonton, Canada, June 1979.

20. Elwi, A.A., and Murray, D.W., "A 3D Hypoelastic Concrete Constitutive Relationship", Journal of the Engineering Mechanics Division, American Society of Civil Engineers, New York, August 1979.

21. Elwi, A.A., "Nonlinear Analysis of Axisymmetric Reinforced Concrete Structures",Ph.D. Thesis, Department of Civil Engineering, University of Alberta , Edmonton, Alberta, Apring, 1980.

Other References

22. Bushnell, D., "Stress, Stability and Vibration of Complex Branched Shells of Revolution: User's Manual for BOSOR4", Lockheed Missile and Space Company, Inc., Sunnyvale, California.

23. Bushnell, D., "BOSOR5 - A Computer Program for Buckling of Elastic-Plastic Complex Shells of Revolution Incuding Large Deflections and Creep; Vol. 1: User's Manual, Input Data", Lockheed Missiles and Space Company, Inc., Sunnyvale, California, December, 1974.

24. Beeby, A.W., "A Study of Cracking in Reinforced Concrete

Members Subjected to Pure Tension", Technical Report 42.468, Cement and Concrete Association, London, June 1972.

25. Leonhardt, F.; "Crack Control in Concrete Structures", IABSE Surveys, S-4/77, IABSE Periodical 3/1977, International Association for Bridge and Structural Engineering, Zurich, August 1977.